LUND UNIVERSITY

User Effect Mitigation in MIMO Terminal Antennas

Vasilev, Ivaylo

2015

User Effect Mitigation in MIMO Terminal Antennas

Doctoral Dissertation

Ivaylo Vasilev

Lund University
Lund, Sweden
2015

Department of Electrical and Information Technology
Lund University
Box 118, SE-221 00 LUND
SWEDEN

This thesis is set in Computer Modern 10pt
with the LaTeX Documentation System

Series of licentiate and doctoral theses
No. 70
ISSN 1654-790X
ISBN 978-91-7623-284-2

...to my exceptionally devoted and loving mother...

"It ain't about how hard you hit, it's about how hard you can get hit and keep moving forward" - Rocky Balboa

Popular Science Summary

In recent years, the use of smartphones for Internet access, video streaming and other exciting services is fundamentally transforming the way we live and work. Some latest figures indicate that the number of smartphone users is expected to exceed 2 billion by 2016. However, one key limitation of smartphone performance is still an open research question: it has been shown that the inevitable proximity of users significantly impairs smartphone antennas' capability to transmit and receive signals, resulting in lower Internet speeds, dropped calls and reduced battery life. This thesis investigated methods for mitigating user effects on the performance of multi-antenna mobile terminals in the context of future wireless communication networks such as Long Term Evolution Advanced (LTE-A). Firstly, to account for the increasing size of terminal devices as well as the variety of new usage scenarios in smartphone application, 11 representative user scenarios were designed to study user-induced antenna impairments in handsets with different antenna designs. The results offer some guidelines for designing efficient terminal antennas in the presence of users. Secondly, to provide user effect mitigation beyond a fixed antenna configuration, the thesis performed a comprehensive study of applying adaptive impedance matching (AIM) as a potential solution. Moreover, AIM was also investigated with respect to its ability to improve terminal performance by optimizing the interaction between the terminal antenna and the propagation environment. A systematic approach was taken to study AIM, where the initial step was to determine the possible performance gains based on computer simulations of ideal setups. Then, the ideal setups were progressively relaxed through experiments involving real terminal antennas, tuners, users and propagation environments, where each step provided insights for further work. For example, the small integrated tuners used in this work were designed based on the characteristics of the antenna impedance in the measured scenarios. Detailed experimental studies confirmed that AIM can provide significant equivalent net power gain of up to 2.5 dB. Apart from technical papers, one important end product of this thesis is a technology demonstrator that can display the effectiveness of

the proposed AIM solution in real time.

Abstract

The rapid growth of cellular technology over the past decade transformed our lives, enabling billions of people to enjoy interactive multimedia content and ubiquitous connectivity through a device that can fit into the palm of a hand. In part the explosive growth of the smartphone market is enabled by innovative antenna system technologies, such as multiple-input multiple-output (MIMO) systems, facilitating high data rates and reliable connections. Even though future deployment of Long Term Evolution Advanced (LTE-A) is expected to provide seamless internet connectivity at even higher speeds over a wide range of devices with different form factors, fundamental terminal antenna limitations can severely impact the actual performance of the terminal. One of the key challenges in terminal antenna design are user-induced losses. It has been shown that electromagnetic absorption in body tissues as well as antenna impedance mismatch due to user proximity significantly degrade terminal antenna performance. Moreover, user interactions are non-static, which further complicates terminal design by leading to the requirement of evaluating a wide range of hand grips and usage scenarios. This doctoral thesis explores these challenges and offers useful insight on effective user interaction mitigation. In particular, state-of-the-art multiple antenna designs have been investigated in an attempt to formulate guidelines on efficient terminal antenna design in the presence of a user (Paper I). Moreover, the major part of the thesis considers the method of adaptive impedance matching (AIM) for performance enhancements of MIMO terminals. Both ideal and very practical and realistic AIM systems have been studied in order to extend the knowledge in the area by determining achievable performance gains and providing insights on AIM gain mechanisms for different terminal antenna designs, propagation environments and user scenarios.

In Paper I, five different MIMO terminal antenna designs were evaluated in 11 representative user scenarios. Two of the prototypes were optimized with the Theory of Characteristic Modes (TCM), whereas the remaining three were based on more conventional antenna types. Multiplexing efficiency (ME)

was used as the MIMO system performance metric, assuming an ideal uniform 3D propagation environment. The paper focuses on performance at frequency bands below 1 GHz due to the more stringent size limitations.

Paper II presents a simulation model of the complete physical channel link based on ideal lossless AIM and evaluates the potential of AIM to mitigate user effects for three terminal antennas in four user scenarios. The prototypes studied have different performances in terms of bandwidth and isolation. MIMO capacity was used as the main performance metric. In order to gain insight on the impact of terminal bandwidth, as well as system bandwidth on AIM performance, capacity calculations were performed both for the center frequency and over the full LTE Band 13.

In Paper III, a practical AIM system was set up and measured in both indoor and outdoor propagation scenarios for a one-hand and a two-hand grip, including a torso phantom. The AIM system consisted of two Maury mechanical tuners controlled with LabView. MIMO capacity was used to determine performance in the different user and channel cases. The impact of different propagation environments and user cases was discussed in detail. Moreover, tuner loss estimation was done to enable the calculation of AIM net gains.

In Paper IV, the simulation model from Paper II was extended to include real antenna parameters as well as simulated environments with non-uniform angular power spectra. Two fundamentally different antenna designs were measured in three user scenarios involving phantom hands, whereas non-uniform environments of different angular spreads were simulated in post-processing. The study presents results and analysis on the impact of user scenarios and environment on the AIM gains for the terminals with different antenna designs.

Finally, Paper V describes a realistic AIM system with custom-designed CMOS-SOI impedance tuners on a MIMO terminal antenna. Measurement setup control, as well as MIMO system evaluation, was achieved through a custom-developed LabView software. Detailed propagation measurements in three different environments with both phantom users and real test subjects were performed. The analysis and discussions provided insights on the practical implementation of AIM as well as on its performance in realistic conditions.

Preface

This doctoral thesis concludes my work as a PhD student at the Department of Electrical and Information Technology, Lund University, and is comprised of two parts. The first part provides an overview of the research field and summarizes the main scientific contributions, whereas the second part comprises five research papers in their published or submitted format. The included research papers are:

[1] I. Vasilev and B. K. Lau, "On user effects in MIMO handset antennas designed using characteristic modes," submitted to *IEEE Antennas and Wireless Propagation Letters*, Mar. 2015.

[2] I. Vasilev, E. Foroozanfard, and B. K. Lau, "Adaptive impedance matching performance of MIMO terminals with different bandwidth and isolation properties in realistic user scenarios," in *Proc. European Conference on Antennas and Propagation*, Gothenburg, Sweden, Apr. 8-12, 2013, pp. 2590-2594.

[3] I. Vasilev, V. Plicanic, R. Tian, and B. K. Lau, "Measured adaptive matching performance of a MIMO terminal with user effects," *IEEE Antennas and Wireless Propagation Letters*, pp. 1720-1723, 2013.

[4] I. Vasilev, V. Plicanic, and B. K. Lau, "Impact of antenna design on MIMO performance for compact terminals with adaptive impedance matching," in revision for *IEEE Transactions on Antennas and Propagation*, Jun. 2014.

[5] I. Vasilev, J. Lindstrand, V. Plicanic, H. Sjöland, and B. K. Lau, "Experimental investigation of adaptive impedance matching for a MIMO terminal under realistic conditions," submitted to *IEEE Transactions on Antennas and Propagation*, Mar. 2015.

During my PhD studies, I have also contributed to the following publications. However, these publications are not included in the thesis:

[6] J. Lindstrand, I. Vasilev, and H. Sjöland, "A low band cellular terminal antenna impedance tuner in 130nm CMOS-SOI technology," in *Proc. European Solid State Circuits Conference*, Venice, Italy, Sep. 22-26, 2014, pp. 459-462.

[7] I. Vasilev, V. Plicanic, R. Tian, and B. K. Lau, "Experimental study of adaptive impedance matching in an indoor environment," in *Proc. IEEE International Symposium on Antennas and Propagation*, Memphis, TN, Jul. 6-11, 2014, pp. 685-686.

[8] I. Vasilev, V. Plicanic, and B. K. Lau, "On user effect compensation of MIMO terminals with adaptive impedance matching," in *Proc. IEEE International Symposium on Antennas and Propagation*, Orlando, FL, Jul. 7-13, 2013, pp. 174-175.

[9] V. Plicanic, I. Vasilev, R. Tian, and B. K. Lau, "Capacity maximisation of handheld MIMO terminal with adaptive matching in indoor environment," *Electronics Letters*, vol. 47, no. 16, pp. 900-901, Aug. 2011.

The research results throughout my graduate study have also been presented as temporary documents (TDs) in the European Cooperation in Science and Technology (COST) Action IC1004:

[10] I. Vasilev, V. Plicanic, R. Tian, and B. K. Lau, "Field measurement performance of a MIMO terminal with adaptive impedance matching," in *COST IC1004*, TD(14)09050, Ferrara, Italy, Feb. 2014.

[11] I. Vasilev, V. Plicanic, and B. K. Lau, "Comparison of performance benefits from adaptive impedance matching for two MIMO terminals under a two-hand scenario," in *COST IC1004*, TD(13)07033, Ilmenau, Germany, May 2013.

[12] I. Vasilev, E. Foroozanfard, and B. K. Lau, "On the performance of adaptive impedance matching in MIMO terminals with different antenna characteristics," in *COST IC1004*, TD(13)06069, Malaga, Spain, Feb. 2013.

Acknowledgements

It is foolish to believe a man stands on his own during defining moments in life. My PhD studies were filled with such moments and I am glad to have always had the support of family, friends, and colleagues. I am truly grateful to all of them and I will never forget their sacrifices, their help, their advice and their criticism when I needed it the most.

First and foremost, I would like to express my sincere gratitude to my advisor, Assoc. Prof. Buon Kiong Lau for believing in me and for providing me with the opportunity to pursue a PhD under his supervision. His relentless pursuit of academic and professional excellence has been a true inspiration and a life-long lesson on how to approach my future career development. I am truly grateful for the countless hours he invested in perfecting my manuscripts and discussing the latest results on our projects. His attention to detail and extensive knowledge in the field have truly guided me to become a better researcher.

Secondly, I am grateful to all the amazing colleagues that I had the privilege to work with. Dr. Ruiyuan Tian, Dr. Vanja Plicanic Samuelsson, Dr. Hui Li and Zachary Miers showed a great deal of kindness and support throughout countless meetings, discussions and many hours of measurements. I was and still am very impressed with the devotion, precision and high efficiency with which you approach your work. Many other colleagues also contributed greatly during my studies in Lund. I would like to thank Jonas Lindstrand and my co-supervisor Prof. Henrik Sjöland for the valuable discussions and countless hours spend in the lab. I would also like to express my sincere gratitude to Dr. Peter C. Karlsson, Dr. Vanja Plicanic Samuelsson, Thomas Bolin, Zhinong Ying, and Erik Bengtsson from Sony Mobile Communications AB for supporting our measurement campaigns and providing valuable insight on my results at numerous meetings. Many thanks to Assoc. Prof. Buon Kiong Lau, Prof. Mats Gustafsson, Prof. Fredrik Tufvesson, Prof. Henrik Sjöland, Assoc. Prof. Markus Törmänen and Göran Jönsson for teaching me about multiple antenna systems, propagation channels, RF circuits and measurement techniques. A special thank you also goes to all my past and current fellow PhD students

at the department for sharing research ideas and collaborating in our teaching activities. I sincerely thank Lars Hedenstjerna for his engineering support on many occasions. Thanks to Max Landaeus for providing free license to the BetaMatch software. I am also grateful to my master students Ehsan Foroozanfard, Hayder Al-Zubaidi and Baydai Abdulameer for contributing to some of my papers. Thanks to Pia Bruhn, Doris Glöck, Elisabeth Nordström, Birgitta Holmgren, Anne Andersson, Josef Wajnblom, Bertil Lindvall and Robert Johnsson for taking care of administrative matters and for providing critical IT support.

I would also like to thank Prof. Gert Frølund Pedersen for taking the time to be the faculty opponent of my thesis, Prof. Mark Beach, Prof. Katsuyuki Haneda, Adjunct Prof. Jan Carlsson, and Dr. Dmytro Pugachov for agreeing to be the grading committee members.

I am also truly grateful to Prof. Jon W. Wallace for encouraging me to pursue a PhD and for believing I have what it takes to succeed in the academic field. Moreover, I am fortunate to have a great mentor in the PLUME program. Thank you to Katarina Strömberg for the valuable career advice during the past year in the program.

Many friends have been supportive during my PhD studies. I am very grateful to Tsvetan Bratoev, Fabio Pereira, Walan Grizolli, Dimitrios Vlastaras, Zachary Miers, Karl-Magnus Persson, Anders Bernland, Reza Meraji, Rohit Chandra, Taimoor Abbas and Farzad Foroughi. In football terms you guys have been a tremendous support on and off the field and I truly appreciate it. Special thank you to Tsvetan Bratoev for being a true friend and partner in crime for more than 17 years. I am also extremely grateful you never let me forget how much I love my homeland. At this point I would like to say a special thank you to my girlfriend Desislava Halova. For the past 2.5 years you have been an amazing support. Thank you for your genuine love, patience and understanding during what has been the harder part of my PhD studies.

Finally, my endless gratitude, love and respect go to my family for their sacrifices and limitless support during the past ten years of my studies abroad. In particular, I am sincerely grateful to my mother Valentina Pesheva. In all my life I have been truly mesmerized by your devotion and true love. You have been a tremendous support in all my endeavors and always believed in me. There are no words that can do justice to how much I cherish you. This thesis would have never been possible without you!

This work has been financially supported by VINNOVA (Grant no. 2009-02969) and in part by Sony Mobile Communications AB in Lund. Travel grants from Kungliga Fysiografiska Sällskapet in Lund and Ericsson Research Foundation are also greatly appreciated.

Ivaylo Vasilev

List of Acronyms and Abbreviations

2D Two Dimensional

3D Three Dimensional

AIM Adaptive Impedance Matching

AOA Angle-of-Arrival

APS Angular Power Spectrum

AS Angular Spread

CCE Capacitive Coupling Element

CTIA Cellular Telecommunications Industry Association

D2D Device-to-Device

DTC Digitally Tunable Capacitor

ED Eigenvalue Dispersion

EM Electromagnetic

ES Ellipticity Statistic

FDTD Finite-Difference Time-Domain

FEM Finite Element Method

FOM Figure of Merit

FS Free Space

IEEE Institute of Electrical and Electronics Engineers

IFA Inverted-F Antenna

IFBW Intermediate Frequency Bandwidth

IID Independent and Identically Distributed

HSPA High Speed Packet Access

LNA Low Noise Amplifier

LOS Line-of-Sight

LTE Long Term Evolution

LTE-A Long Term Evolution Advanced

ME Multiplexing Efficiency

MEG Mean Effective Gain

METIS Mobile Enablers for the Twenty-Twenty Information Society

MIMO Multiple-Input Multiple-Output

MMC Massive Machine Communication

MPC Multipath Component

NLOS Non-Line-of-Sight

OH One-Hand

OTA Over-the-Air

PCB Printed Circuit Board

PDC Personal Digital Cellular

PIFA Planar Inverted-F Antenna

RF Radio Frequency

RX Receiver

SAR Specific Absorption Rate

SISO Single-Input Single-Output

SM Spatial Multiplexing

SNR Signal-to-Noise Ratio

SVD Singular Value Decomposition

TCM Theory of Characteristic Modes

TH Two-Hand

TX Transmitter

UART Universal Asynchronous Receive/Transmit

UMTS Universal Mobile Communications System

URC Ultra-Reliable Communication

VNA Vector Network Analyzer

VSWR Voltage Standing Wave Ratio

WLAN Wireless Local Area Network

XPD Cross-Polarization Discrimination

ZMCSCG Zero Mean Circularly Symmetric Complex Gaussian

Contents

Part I

Research Field Overview

Chapter 1

Introduction

The advances in electrical engineering over the past two centuries have shaped our society and way of life to a point where access to wirelessly transmitted information is ubiquitous in both our personal and professional lives. A number of outstanding scientists, engineers and visionaries have contributed to the final products our generations have been so fortunate to enjoy. This chapter aims to guide the reader from a few of the fundamental discoveries in the past to a vision of future mobile communications, as well as to provide the scope and goals of this doctoral thesis.

1.1 Historical Background

Even though Heinrich Hertz himself saw no practical use of his work on the transmission and reception of electromagnetic waves, his experiments in the late 19^{th} century were one of the first practical demonstrations of wireless communication. A few decades later, in the beginning of the 20^{th} century, an Italian inventor and electrical engineer, Guglielmo Marconi, took a more entrepreneurial approach and founded The Wireless Telegraph & Signal Company with a dream to achieve wireless transmission over the Atlantic Ocean. In 1901 Marconi successfully transmitted the letter "S" in Morse code from Cornwall (now part of the United Kingdom) to Newfoundland (now part of Canada). These and many other experiments conducted in the beginning of the 20^{th} century marked the beginning of wireless communications.

The initial success of Marconi's experiments paved the way for future work, but it only showed a glimpse of the vast potential of wireless communications. It was not until Bell Laboratories developed the cellular concept in the 1960s

when the vision of personal wireless services was born [1]. Later, the advances in solid-state RF hardware in the 1970s unlocked the practical implementation of the cellular concept and led to the exponential growth of cellular technology in the next three decades [1].

Figure 1.1: IBM Simon next to an Apple iPhone 4s [2].

It took nearly 20 years of personal device evolution before the first smartphone was born. In 1994 the IBM Simon Personal Communicator was released. In Fig. 1.1 it is shown next to a contemporary device (the 2011 Apple iPhone 4s) [2]. Simon supported functionalities well ahead of its time. It had a touchscreen display, e-mail capabilities, calendar, address book, calculator and a sketch pad [3]. Yet, for the six months it was available on the market only 50,000 units were sold. Even though customers had a device capable of consuming huge amounts of wirelessly transmitted data, cellular networks had some catching up to do. At the time cellular networks were designed mainly for voice, not data transmission. Moreover, only limited content was digitally available and there were no third party programs. These drawbacks essentially limited Simon's vast potential and put the smartphone concept on the shelf for another decade.

The next and arguably the most significant step in wireless personal device evolution was made by Apple in January 2007, when the first iPhone was announced. The then Apple CEO, Steve Jobs, and his colleagues are credited with the way they challenged our perception of mobile phones by combining the functionalities of a conventional voice-call phone, music player and an internet communication device in one product. Even though many other devices shared

similar functionalities, the iPhone package was so appealing to the customer that it quickly became a huge success and skyrocketed Apple to the top of the most valuable brands in the world. The company sold 6.1 million units of its first generation iPhone, and this number continues to grow dramatically for subsequent versions of the smartphone.

1.2 Future of Wireless Communications

The announcement of the iPhone triggered intensive software and hardware product development in competing companies, resulting in an unprecedented era of growth in the wireless communications field. Network operators rushed to provide fast and reliable connection for all subscribers, while smartphone manufacturers came up with faster, slimmer, and more feature-rich devices. This race continues today with even higher demands for smartphones predicted for the next 5 years. According to Statista [4], a linear increase in global smartphone shipments is forecasted in the period 2010-2018. Figure 1.2 shows that the expected units shipped are to increase from 1.2 billion in 2014 to 1.7 billion in 2018. Moreover, with every subsequent smartphone generation user expectations for performance and quality of service increase. Therefore, designing and building future generation networks and devices becomes more and more challenging.

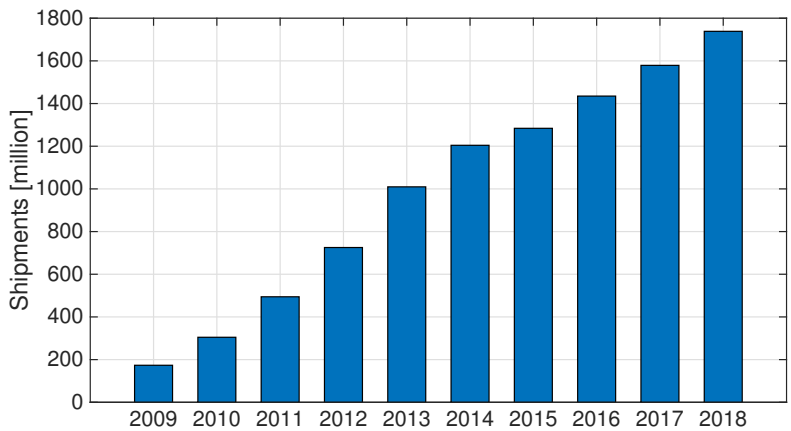

Figure 1.2: Global smartphone shipments forecast [4].

Existing state-of-the-art wireless networks, such as Long Term Evolution (LTE) and Institute of Electrical and Electronics Engineers (IEEE) 802.11ac Wi-Fi, provide reliable wireless services at higher data rates as compared to previous generations' standards. Yet, the emergence of new scenarios and the more stringent requirements on data rate, latency and network volume define the scope of future 5G networks [5]. The 5G vision of the METIS project is presented in Fig. 1.3.

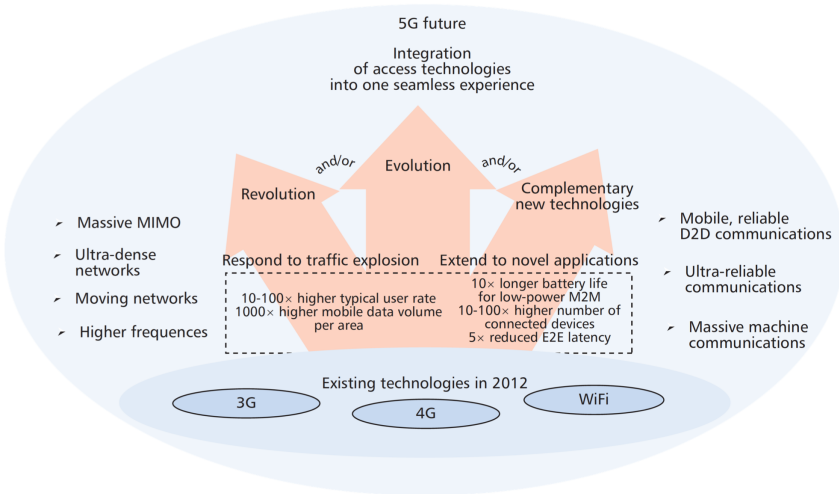

Figure 1.3: METIS project vision for the 5G roadmap [5] ©2014 IEEE.

In the METIS project several key future scenarios have been identified [5]:

- "Amazingly fast" - high data rates for future mobile broadband users
- "Great service in a crowd" - reasonable experience in crowded areas
- "Best experience follows you" - good experience for users on the move (cars, trains etc.)
- "Ubiquitous things communicating" - efficient handling of a very large number of devices (e.g. sensors)

A number of use cases fall into these very broadly defined scenarios. Efficient device-to-device (D2D) and massive machine communication (MMC) can contribute to smarter homes, vehicles and transportation systems, whereas ultra-reliable communication (URC) is the fundamental requirement for full integration of wireless communication in personal and public health services.

Many other recent contributions also emphasize the wide variety of scenarios and technologies relevant for future 5G networks. The authors in [6] discuss the multi-tier nature of upcoming 5G architectures (see Fig. 1.4), presented as multiple communication scenarios within macrocells including smaller pico and femtocells as well as D2D communication. The coexistence of all scenarios increases the complexity of interference management and device awareness, thus presenting further technological challenges to 5G network realization.

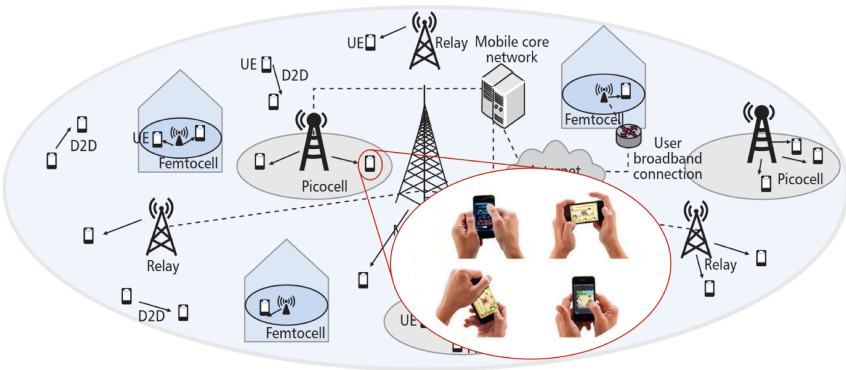

Figure 1.4: Multi-tier network (macrocells, picocells, femtocells, relays, and D2D links) with terminals in various hand grips [6].

In [7] a detailed discussion of state-of-the-art 5G research and initiatives is presented focusing on key technologies, challenges and their regulation and standardization. In order to handle all scenarios and use cases future wireless networks are expected to achieve 1000 times higher data volume per area for 10 to 100 times more connected devices, while offering reduced end-to-end latency, longer battery life and increased network reliability. It is expected that these stringent requirements will be met in part through the use of massive multiple-input multiple-output (MIMO) technologies, more efficient frequency spectrum usage and standardization, mmWave spectrum utilization, as well as adaptive MIMO handsets. In the context of terminal antennas the main challenges in realizing this grand vision of future 5G networks are:

- Unprecedented number of antenna elements (at least 4 in LTE-A [8])
- High resilience in various user and propagation scenarios (see Fig. 1.4)
- Large operational bandwidth covering existing and future standards
- Low correlation and coupling supporting enhanced MIMO operation

1.3 Thesis Scope and Goals

Broadly, the scope of this dissertation covers the complete radio channel shown in Fig. 1.5. It includes the propagation environment, the antennas and in part the RF (radio frequency) front end up to the frequency conversion stages [9]. In practice wireless transmission and reception is a sophisticated process. In general, it starts with the conversion of analogue information into raw electrical form by sensors. Next, this information is digitized and prepared for transmission in the baseband domain [9]. This includes encoding, filtering and modulation. Finally, the data is converted back from the digital to the analog domain, shifted up in frequency and transmitted via the antenna into the propagation environment [9]. During reception the process is reversed. Each of these steps is a broad research area in itself and involves many design and optimization steps.

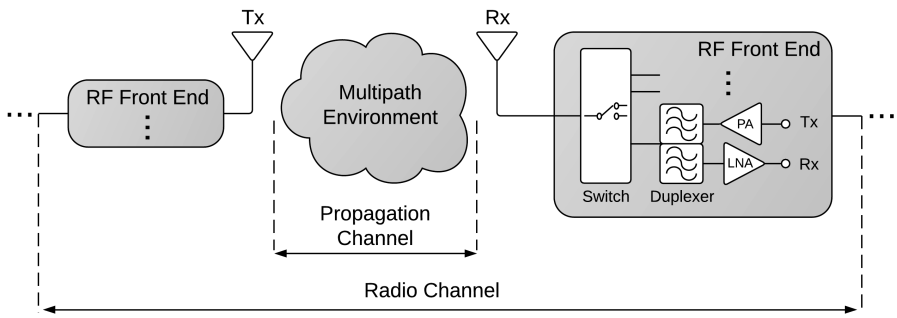

Figure 1.5: Radio channel diagram.

Propagation Channel

The medium in which electromagnetic waves propagate is more generally known as the propagation channel (see Fig. 1.5). It includes all objects (*e.g.*, air, trees, cars, buildings etc.) in the geometrical space where the propagation occurs. Each object in this space contributes with one or multiple propagation paths (thus the common name multipath) to the signal at the receiver antenna, governed by the four main propagation mechanisms (free-space propagation, reflection, diffraction and scattering). Since the exact position, distance and speed of objects in the propagation space are typically non-uniform, new contributions arrive at the receiver with different delays, doppler frequencies, amplitudes and polarizations [9]. All these multiple arrivals represent the full propagation channel. The exact analysis of all arrivals is a complicated endeavor, but

is usually not of primary interest. Efforts of studying propagation are rather invested in the analytical modeling and practical measurement of real world environments. Researchers focus on studying measured data to develop accurate and versatile propagation channel models based on statistical parameters, resulting in an intricate, parameter-dependent transfer function describing the effect of the propagation environment on transmitted signals. This approach facilitates researchers in higher layers to include propagation effects in link and system evaluations.

Antennas

Antennas are responsible for emitting electromagnetic (EM) waves in the propagation environment and are therefore crucial for successful wireless transmissions. Key factors in designing antennas are efficiency, directivity, polarization, bandwidth and size, whereas optimum designs are often tradeoffs between these crucial parameters depending on the requirements of the system. In the context of handsets the size and bandwidth requirements are so stringent that often efficiency is sacrificed to fulfill specifications. Moreover, due to their application, terminal antennas are required to operate in challenging conditions for efficient EM wave propagation such as close proximity to biological tissues (user's body) and random propagation environments.

RF Front End

Circuit components immediately after the antenna, in the receiver chain, are commonly referred to as the RF front end. The bridge to the antenna elements is often realized through impedance matching components. Future state of the art implementations are expected to include adaptive tuning modules targeting mismatch compensation or frequency reconfiguration. Following any tuning modules are a switch, duplexers and amplifiers as shown in Fig. 1.5. An antenna switch's main functionality is to selectively connect the antenna element to the corresponding line-ups and thus isolate different RF paths as well as to provide TX (transmit) and RX (receive) separation in GSM (Global System for Mobile Communications) systems [10]. The duplexer consists of two band-pass filters and is used to simultaneously connect the antenna to the TX and RX paths in UMTS (Universal Mobile Communications System) and Long-Term Evolution (LTE) systems while providing sufficient TX/RX isolation [10]. Finally, the power amplifier (PA) is responsible for accurately amplifying the signals applied at its input and delivering power to the antenna in the TX mode of operation. Its function is crucial as this is one of the components consuming most power in the RF chain. Therefore, optimal operation

and excellent output matching are crucial requirements in PA design [10]. The low noise amplifier (LNA) has similar requirements but is used in the RX mode and focuses on providing maximum amplification at minimum noise figure.

Thesis Scope

In the context of the above description, the scope of the research work carried out in this thesis addresses the need for highly efficient, user-resilient MIMO terminal antenna solutions reliable in various propagation environments. An interdisciplinary approach was taken in an attempt to combine existing knowledge with novel ideas in the areas of antennas, propagation and circuit design to study, optimize and experimentally verify antenna system performance in realistic propagation and user scenarios. Adaptive impedance matching (AIM) was evaluated through analytical and experimental studies as a performance enhancement technology in the presence of unfavorable user and propagation conditions. In addition, fundamentally different MIMO terminal antenna designs were evaluated to gain insight on user-robust antenna design and its impact on MIMO performance.

Project Goals

The goals of this dissertation work are to:

- Perform detailed simulation and measurement studies of user effects on terminal antenna performance employing both standard phantoms and real user test subjects (Papers I – V).

- Draw conclusions on user-robust terminal antenna designs based on studies of fundamentally different MIMO terminals antennas (Papers I, II, and IV).

- Establish and quantify the potential of AIM to improve system performance by investigating both ideal tuner networks as well as practical tuner solutions (Papers II – V).

- Investigate the effect of antenna design on AIM performance via studies with fundamentally different terminal prototypes and outline the key antenna parameters with significant influence on AIM (Papers II and IV).

- Perform detailed analytical studies and experimentally verify the effects of the propagation environment on AIM potential (Papers III – V).

- Design and build a complete AIM testbed including custom-designed tuners, MIMO terminal antenna and performance evaluation software in order to demonstrate real-time AIM performance improvements in a realistic propagation environment (Chapter 5 and Paper V).

Chapter 2

MIMO Systems

MIMO is a driving technology enabling the unprecedented growth of data rate and reliability in mobile communications over the past decades [11]. Some of the most widely used wireless standards today, such as LTE and IEEE 802.11ac Wi-Fi, require multiple antenna modes of operation, whereas upcoming standards (*e.g.*, LTE-A) rely on implementations of more than two cellular antenna elements in handsets in order to reach the target 1 Gbps data rate [8]. The scope of this chapter is to present fundamentals of MIMO wireless communications relevant to the work carried out in this doctoral thesis. The signal model of multiple antenna systems used is initially presented. Next, several propagation channel models are introduced and finally, performance characterization metrics relevant to antenna and system performance are discussed.

2.1 Introduction

In traditional single-input single-output (SISO) linear systems, one TX antenna and one RX antenna are used for communication, whereas the propagation environment is commonly represented by the channel impulse response which is a function of both time (t) and delay (τ) - $h(t,\tau)$. It represents the summation of energy from all paths in the physical channel. For a time and frequency invariant system the dependence on t and τ is dropped and the channel representation becomes a complex scalar number, h. These assumptions hold for narrow band systems in a static environment, which is the default propagation setup used throughout this thesis. In such conditions the received signal can be expressed as

$$y = hx + n, \tag{2.1}$$

where y is the received signal, h is the channel impulse response, x is the transmitted signal and n is the additive white Gaussian noise (AWGN) [12]. The spectral efficiency of such a channel to support communication between the TX and RX is upper bounded by the Shannon capacity, which can be expressed in bits per second per Hertz (bits/s/Hz) as

$$C = \log_2 \left(1 + \frac{P_T}{\sigma_n^2}|h|^2\right), \tag{2.2}$$

where P_T is the transmit power, σ_n^2 is the noise variance, and $|h|^2$ is the gain of the scalar SISO channel. As seen in (2.2) in order to increase the total amount of information transferred through the SISO channel we can either increase the bandwidth of the system, or increase the transmit power. Neither of these solutions are viable due to the densely populated frequency spectrum of current wireless systems and the energy efficiency requirements limiting the available total transmit power.

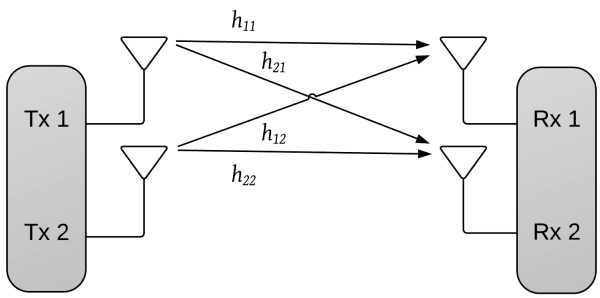

Figure 2.1: 2×2 MIMO downlink channel.

Fortunately, multiple antenna systems offer an alternative solution. A MIMO system employs multiple antennas on both the transmit and receive sides of the communication link. The setup in Fig. 2.1 presents a 2×2 MIMO link, which is the default MIMO configuration used in this thesis, in compliance with LTE requirements of at least two antennas on both sides of the communication system [8]. In this setup the impulse response of the channel will be expressed as a 2×2 matrix $\mathbf{H}$ whose elements denote the scalar SISO channels formed between each pair of TX / RX antennas. The simplified signal model is then given by

$$\boldsymbol{y} = \mathbf{H}\boldsymbol{x} + \boldsymbol{n}, \tag{2.3}$$

where $\boldsymbol{y}$ is the received signal vector, $\boldsymbol{x}$ is the transmit signal vector, and $\boldsymbol{n}$ is the noise vector modeled as AWGN. The capacity of such a MIMO system with no channel state information at the TX has been derived in [12, 13] and can be expressed as

$$C = \log_2 \det \left(\mathbf{I}_{M_R} + \frac{P_T}{M_T \sigma_n^2} \mathbf{H}\mathbf{H}^H \right), \tag{2.4}$$

where $\mathbf{I}_{M_R}$ is the $M_R \times M_R$ identity matrix (2×2 in the example in Fig. 2.1), M_T is the number of transmit antennas (2 in the example in Fig. 2.1), P_T is the transmit power evenly distributed among all transmit elements, $\det(\cdot)$ is the determinant operator and $(\cdot)^H$ is the Hermitian operator. Assuming an orthogonal MIMO channel matrix $\mathbf{H}$ and $M_T = M_R = M$ it has been shown in [12, 13] that (2.4) simplifies to

$$C = M \log_2 \left(1 + \frac{P_T}{\sigma_n^2} \right), \tag{2.5}$$

The fundamental derivation in (2.5) implies that capacity scales linearly with the number of antenna elements without sacrificing the limited resources of bandwidth and transmit power. This enables a significant increase in information transfer as compared to conventional SISO systems. Beyond the increase in spectral efficiency, MIMO systems are credited with increasing reliability and coverage in mobile communications through diversity and beamforming techniques.

In diversity mode, MIMO systems transmit multiple copies of the same signal through all transmit antennas in an effort to minimize fading effects at the receiver and therefore improve reliability. Depending on the antenna design and position we distinguish between angle, polarization and spatial diversity. As the name suggests, we can exploit either angle, polarization or spatial independence in the transmitted signals in order to improve the fading characteristics of the channel. With beamforming, MIMO systems aim at increasing SNR and reducing interference through forming more directive antenna system radiation, hence improving reliability and coverage.

This brief discussion emphasizes the massive potential of multiple antenna systems to improve spectral efficiency and system reliability. Yet, it has been shown that the structure of the MIMO channel matrix $\mathbf{H}$ is critical in realizing these benefits. Hence, tremendous efforts have been spent in the past decades to better understand and model MIMO channels in order to fully take advantage of their spatial characteristics.

2.2 Propagation Channel Models

Efforts in MIMO channel modeling focus on accurate and computationally inexpensive representations of the MIMO channel impulse response. Yet, depending on the approach we distinguish between two different categories of channel models, namely analytical and physical.

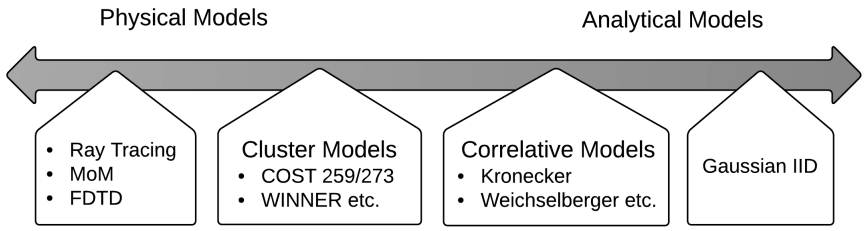

Figure 2.2: Spectrum of channel models [14].

Figure 2.2 shows the spectrum of MIMO channel models depending on which broad category they fall into. The channel models on the far left of the diagram are much more related to the physics of electromagnetic (EM) wave propagation. Some of them, such as Finite-difference time-domain (FDTD), solve Maxwell's equations for specific environments and boundary conditions. These are the most accurate models but are only used on a small scale due to the extreme computational requirements needed for applications in larger scale problems. Others, such as Ray Tracing consider fundamental EM propagation mechanisms (free-space propagation, reflection, scattering, diffraction etc.) and the exact geometry of objects in the environment to model the channel [14].

Next, in Fig. 2.2 are cluster channel models. They employ, rays called multipath components (MPCs) to represent the energy contributions at the receiver resulting from reflections, scattering or diffraction. In such models MPCs are grouped into clusters and modeled stochastically based on parameters such as time of arrival and level of attenuation measured in real-life systems. Cluster models are widely applied in practice due to their flexibility and ease of use.

The last two groups of channel models are the purely stochastic Gaussian independent and identically distributed (IID) model and the correlative models, such as the Kronecker model. In this case only the spatial structure of the channel is considered by modeling the correlation between different propagation paths in the MIMO channel. Throughout this thesis both the Gaussian IID and Kronecker models have been widely applied to evaluate MIMO systems analytically. Yet, several propagation channel measurement campaigns were also performed in order to estimate real-life performance.

Gaussian IID Channel Model

Depending on the presence of a dominant deterministic propagation path between the TX and RX we distinguish between non-line-of-sight (NLOS) and line-of-sight (LOS) propagation. NLOS scenarios are traditionally representative of rich scattering environments where individual SISO links in the MIMO channel matrix $\mathbf{H}$ can be modeled as independent zero mean circularly symmetric complex Gaussian (ZMCSCG) random variables. ZMCSCG is a special case of a complex random variable where both the real and imaginary components are independent real Gaussian random variables with zero mean and equal variance [12]. This channel model is widely known as the Gaussian IID model. We denote the MIMO IID Gaussian channel matrix as $\mathbf{H}_{\text{IID}}$. In this setup the amplitude of each SISO sub-channel $|[\mathbf{H}_{\text{IID}}]_{ij}|$ between the *i-th* receive antenna and *j-th* transmit antenna, is Rayleigh distributed, whereas the phase is uniformly distributed between 0 and 2π [15]. According to the above discussion all sub-channels satisfy the following properties:

$$\mathbb{E}\{[\mathbf{H}_{\text{IID}}]_{ij}\} = 0, \tag{2.6}$$

$$\mathbb{E}\{|[\mathbf{H}_{\text{IID}}]_{ii}|^2\} = 1, \tag{2.7}$$

$$\mathbb{E}\{[\mathbf{H}_{\text{IID}}]_{ij}[\mathbf{H}_{\text{IID}}]^*_{mn}\} = 0, \tag{2.8}$$

where $i \neq m$ or $j \neq n$ and $\{\cdot\}^*$ denotes the complex conjugate operator [12]. These properties imply that the Gaussian IID MIMO channel matrix $\mathbf{H}_{\text{IID}}$ comprises of linearly independent columns resulting in a full rank channel matrix, which is a favorable channel state for MIMO systems.

In LOS scenarios where a dominant propagation path exists between the TX and RX the sub-channel amplitude is typically modeled by a Rician distribution. The Rician K-factor is used to represent the significance of the dominant MPC and is expressed by the ratio of the power in the dominant component to the power of the scattered components. The extreme case when $K \to 0$ implies there is no dominant component and the Rician distribution reduces to a Rayleigh distribution *i.e.*, a NLOS scenario. It has been shown in [12] that deterministic components can be added to the Gaussian IID model to represent LOS scenarios.

Kronecker Channel Model

Correlation between MPCs in the propagation channel or between antennas at the TX or RX is an ever present concern in practical systems and is not taken into account in the Gaussian IID model. One of the simplest and most widely used analytical channel models to consider spatial correlation is the Kronecker channel model. It uses one-sided correlation matrices at the RX and TX to introduce correlation effects to the Gaussian IID model and can be expressed as follows [14]

$$\mathbf{H}_{\mathrm{K}} = \mathbf{R}_{\mathrm{RX}}^{1/2} \mathbf{H}_{\mathrm{IID}} (\mathbf{R}_{\mathrm{TX}}^{1/2})^{T}, \tag{2.9}$$

where $\mathbf{R}_{\mathrm{RX}}$ and $\mathbf{R}_{\mathrm{TX}}$ are the RX and TX one-sided correlation matrices. Yet, the simplicity of the model also leads to deficiencies in certain conditions [16]. The fundamental assumption on the validity of the model is that scatterers around the transmitter are uncorrelated with the ones around the receiver. In other words, the model is valid only if no direct link interacting between the two local scattering environments exists. Scenarios with large separation between the TX and RX fall in this category since the larger the TX/RX separation the higher the probability of having uncorrelated scattering effects around the TX and RX [14]. Generally, the large separation between handsets and base stations (BS) makes the model applicable for mobile terminal communications.

Traditionally, the Gaussian IID channel model and respectively the Kronecker model are used in combination with Monte Carlo simulations over a large number of channel realizations for statistically significant results. This approach was employed in two of the scientific contributions in this thesis, namely [17] (Paper II) and [18] (Paper IV).

Angular Power Spectrum Modeling

Another important aspect of propagation channel modeling relevant to antenna evaluation is the distribution and spread of the angular power spectrum (APS). The APS describes the angular distribution of MPCs incident on the antennas. It can be expressed as

$$P_{\theta,\phi}(\Omega) = P_{\theta}(\Omega)\hat{\theta} + P_{\phi}(\Omega)\hat{\phi}, \tag{2.10}$$

where $P_{\theta}(\Omega)$ and $P_{\phi}(\Omega)$ are the θ- and ϕ-polarization components of the mean incident APS, respectively and $\Omega = (\theta, \phi)$ [19]. Uniform, Laplacian and Gaussian distributions have been widely used to model the incident fields and are also part of standard channel models. In this work both a Gaussian distribution and a uniform 3D distribution have been used to investigate the effect of

a narrow APS on antenna performance. The following expressions show the analytical model used for the incident field:

$$P_{\theta,\phi}^{Uniform}(\theta,\phi) \propto constant, \tag{2.11}$$

$$P_{\theta,\phi}^{Gaussian}(\theta,\phi) \propto \exp\left[-\left(\frac{(\theta-\theta_0)^2}{2\sigma_\theta^2}+\frac{(\phi-\phi_0)^2}{2\sigma_\phi^2}\right)\right], \tag{2.12}$$

where θ_0 and ϕ_0 denote the mean angles-of-arrival (AOA) and σ_θ and σ_ϕ denote the angular spreads (AS) in θ and ϕ polarization respectively [19].

2.3 Performance Characterization

Ultimately, characterizing MIMO system performance is critical in virtually any setup or configuration. Fair, simple and comprehensive figures of merit are key to understanding the full potential of multiple antennas. The following discussion summarizes the main concepts used to evaluate MIMO performance throughout this thesis work.

MEG

The mean effective gain (MEG) was first proposed by Taga [19] and is used to evaluate the effective gain of an antenna system by taking into consideration the APS statistics of the propagation environment. It is defined as the ratio between the mean received power at an antenna and the total mean incident power. According to [9] it can be expressed as

$$\mathrm{MEG_i} = \int\left(\frac{\chi}{1+\chi}G_{\theta,i}(\Omega)P_\theta(\Omega)+\frac{1}{1+\chi}G_{\phi,i}(\Omega)P_\phi(\Omega)\right)\mathrm{d}\Omega, \tag{2.13}$$

where $P_\theta(\Omega)$ and $P_\phi(\Omega)$ are the θ- and ϕ-polarization components of the incident APS as defined in (2.10), $G_{\theta,i}$ and $G_{\phi,i}$ are the θ- and ϕ-polarization components of the *i-th* antenna gain pattern and χ is the cross-polarization discrimination (XPD). The antenna gain pattern ($G_{\theta,\phi}$) and XPD are given by

$$G_{\theta,\phi} = |E_{\theta,\phi}(\Omega)|^2, \tag{2.14}$$

$$\chi = \frac{P_{T,\theta}}{P_{T,\phi}}, \tag{2.15}$$

where $P_{T,\theta}$ and $P_{T,\phi}$ denote the total power of the θ- and ϕ-polarized fields, respectively and $E_{\theta,\phi(\Omega)} = E_\theta(\Omega)\hat{\theta} + E_\phi(\Omega)\hat{\phi}$ is the complex-valued electric far-field pattern. A completely random environment (*i.e.*, isotropic APS or uniform 3D APS) is characterized by $\chi = 1$ and $P_\theta = P_\phi = \frac{1}{4\pi}$. In this case MEG = 1/2, emphasizing that the received power is independent of the antenna gain [9]. In order to account for the realized antenna gain a modified MEG (γ_{i}) expression was suggested in [20]

$$\gamma_{\mathrm{i}} = 2\eta_i \mathrm{MEG_i}, \tag{2.16}$$

where η_i is the total efficiency of the *i-th* antenna port including radiation, mismatch and dielectric losses. Hence, according to (2.16) in a uniform 3D APS $\gamma_{\mathrm{i}} = \eta_{\mathrm{i}}$.

Correlation

Single antenna performance, in terms of MEG, is a crucial power measure for every multiple antenna system positioned in a random APS environment. Yet, it does not provide details on how spatial radiations from different antenna elements are correlated. This information is presented by the complex correlation coefficient, defined in [21]. Similar to the MEG it can be derived for random APS scenarios taking into account both the correlation between antenna radiation patterns and the inherent correlation enforced by the environment's APS. It can be expressed as follows

$$\rho_{\mathrm{c}} = \frac{\int \left(\chi E_{\theta,i} E^*_{\theta,j} P_\theta + E_{\phi,i} E^*_{\phi,j} P_\phi\right) \mathrm{d}\Omega}{\sqrt{\int (\chi G_{\theta,i} P_\theta + G_{\phi,i} P_\phi)\mathrm{d}\Omega \int (\chi G_{\theta,j} P_\theta + G_{\phi,j} P_\phi)\mathrm{d}\Omega}}, \tag{2.17}$$

where $G_{\theta,i}(\Omega)$ and $G_{\phi,i}(\Omega)$ are the θ- and ϕ-polarization components of the *i-th* antenna gain pattern, respectively as in (2.14), $P_{\theta,\phi}(\Omega)$ is the incident APS defined in (2.10), χ is the XPD from (2.15), and $E_{\theta,i}$ and $E_{\phi,i}$ are the θ- and ϕ-polarization components of the complex electric field pattern of the *i-th* antenna. Traditionally, in mobile communications the envelope correlation coefficient is used and according to [9] can be approximated as

$$\rho_e \approx |\rho_c|^2. \tag{2.18}$$

Correlation is known to significantly impair MIMO system performance [12], [14]. It is therefore one of the most crucial figures of merit in multiple antenna systems and of particular importance to a number of research activities in the field as well as to this thesis work.

Channel Gain

In mobile communications, the MIMO channel matrix $\mathbf{H}$ contains information about the TX antennas, the propagation environment, the RX antennas and the terminal user. Therefore, evaluating $\mathbf{H}$ is a common approach to understand system performance. In [14] the quantity $\|\mathbf{H}\|_{\mathrm{F}}^2$ is used to represent the total power gain of the MIMO channel matrix. In this work we employ the total power gain per branch as a received power figure of merit. It can be expressed as

$$G = \frac{\sum_{n=1}^{N} \|\mathbf{H}^{(n)}\|_{\mathrm{F}}^2}{N M_T M_R}, \tag{2.19}$$

where M_T and M_R are the number of transmit and receive antenna elements and N is the number of channel realizations.

Ellipticity Statistic

MIMO system performance is highly dependent on the eigenvalues of the $\mathbf{H}\mathbf{H}^H$ matrix in (2.4) that can be computed from the eigenvalue decomposition

$$\mathbf{H}\mathbf{H}^H = \mathbf{Q}\mathbf{\Lambda}_{eig}\mathbf{Q}^H, \tag{2.20}$$

where $\Lambda_{eig} = \mathrm{diag}[\lambda_1, \lambda_2, ..., \lambda_{\mathrm{k}}]$ is a diagonal matrix containing the eigenvalues of $\mathbf{H}\mathbf{H}^H$. Equally strong eigenvalues enable full utilization of the spatial degrees of freedom provided by multiple antennas [22], whereas significant differences between the eigenvalues result in degraded system performance [12]. In general, the random mixing of MPCs in the propagation environment often results in significant variations among eigenvalues. Hence, eigenvalue dispersion (ED) is of high interest as it directly relates to system performance. Typically, ED is parametrized through the ellipticity statistic (ES) [23], [24] which is evaluated by the ratio of the geometric mean and the arithmetic mean of the eigenvalues (λ_k) from (2.20) as

$$\mathrm{ES} = \frac{\left(\prod_{k=1}^{K} \lambda_k\right)^{\frac{1}{K}}}{\frac{1}{K}\sum_{k=1}^{K} \lambda_k}, \tag{2.21}$$

where K is the rank of $\mathbf{H}\mathbf{H}^H$. High ES implies low eigenvalue dispersion and consequently high channel richness, whereas low ES implies high dispersion

which is an indication of correlated MIMO sub-channels reducing system performance [25].

MIMO Capacity

In this thesis MIMO capacity with no channel state information at the TX was used to evaluate system performance taking into account both propagation and antenna related effects. The system model was built according to (2.3), whereas (2.4) was used for the capacity computations. Yet, different ways of forming the MIMO channel matrix $\mathbf{H}$ were employed in the different scientific contributions throughout this thesis work.

In the simulation studies (Papers II and IV) the Kronecker model (2.9) was used to provide the end-to-end MIMO physical channel. The main focus throughout the thesis was on evaluating downlink MIMO performance, due to the stronger interest to increase data rates in the downlink rather than in the uplink. Hence, for convenience the correlation at the transmit antennas (base station) was assumed to be zero. In this case the end-to-end channel is influenced only by the propagation environment and the RX antennas. Therefore, $\mathbf{R}_{\mathrm{TX}}$ in (2.9) becomes an identity matrix simplifying the Kronecker channel model to the following expression,

$$\mathbf{H} = \mathbf{R}_{\mathrm{RR}}^{1/2}\mathbf{H}_{\mathrm{IID}}, \tag{2.22}$$

where $\mathbf{R}_{\mathrm{RR}}$ is the modified receive correlation matrix according to [26] expressed as

$$\mathbf{R}_{\mathrm{RR}} = \mathbf{\Lambda}^{1/2}\bar{\mathbf{R}}\mathbf{\Lambda}^{1/2}, \tag{2.23}$$

where $\bar{\mathbf{R}}$ is a matrix with ones on the main diagonal and antenna complex correlation coefficient on the off-diagonal elements and $\mathbf{\Lambda}$ is a diagonal matrix with the *i-th* diagonal element representing the total antenna efficiency of the *i-th* antenna. In the propagation channel measurement studies (Papers III and V) the MIMO channel matrix $\mathbf{H}$ was directly measured with a vector network analyzer (VNA). Multiple spatial and frequency samples were measured and used as independent channel realizations in order to provide statistically relevant results.

Multiplexing Efficiency

MIMO performance in the spatial multiplexing (SM) mode of operation *i.e.*, parallel data stream transmission at high SNRs, has been traditionally characterized by capacity in bits/s/Hz. Yet, in many occasions a power related

measure of efficiency is a more intuitive figure of merit for comparing multiple antenna systems operating in the SM mode. In this context, multiplexing efficiency (ME) was proposed in [26] combining antenna correlation and efficiency in a single, intuitive figure of merit. For a 2×2 MIMO setup at high SNRs and in a uniform 3D APS it is expressed as

$$\eta_{me} = \sqrt{\eta_1 \eta_2 (1 - \rho_e)}, \tag{2.24}$$

where η_1 and η_2 are the total antenna efficiencies at port 1 and 2, respectively and ρ_e is the envelope correlation coefficient. For non-uniform propagation scenarios, ME can be calculated using the modified MEG (γ_i) and ρ_c as defined in (2.16), (2.17), and (2.18).

Practical Considerations

The propagation channel models discussed in Chapter 2.2 are ultimately targeted to represent real-life EM propagation as accurately as possible. However, their validity was shown to be subject to various constraints. Hence, propagation measurements are often required to confirm models and verify simulation results. Channel measurements are traditionally performed by a device known as a channel sounder. It transmits electromagnetic waves to excite the channel and records the output at the receiver, thus measuring the channel impulse response $h(t, \tau)$ or channel transfer function $H(t, f)$ depending on the sounding technique used.

In order to measure a MIMO channel three different array architectures can be used: real array, switched array and virtual array [27]. Real array architectures employ as many RF chains as antenna elements, thus severely increasing system cost. Switched array architectures rely on a single RF chain and switch between different antenna elements to measure all sub-channels. Some of the major benefits of the switched array architecture are lower cost and complexity as well as greater flexibility in terms of the size of the MIMO systems that can be characterized. Yet, fast switching between antenna elements is required in order to comply with channel coherence properties. The last architecture is the virtual array, where a single antenna element is connected to a single RF chain. The antenna is then electronically steered to predefined locations in order to emulate a MIMO system and probe individual sub-channels. Even though this technique is cost efficient it only allows for very limited time variations in the channel and does not consider antenna mutual coupling [27].

In this work several measurement campaigns have been performed in both indoor and outdoor propagation environments. In all cases a static environment was enforced. According to the discussion in [28] we ensured minimal

disturbances by (1) using a spectrum analyzer to verify that the frequency band used was not used by other services and (2) limiting movements in the measurement site by restricting access to the measurement area.

In static environments channel sounding can be performed by a VNA since the requirements on the switch speed and sampling rate are lower as compared to time-varying channels. In both Papers III and V a 4-port VNA employing the switched array architecture was used to measure the S-parameter representation of the 2×2 MIMO channel. The intermediate frequency bandwidth (IFBW) of the instrument was set to 2kHz to ensure high noise floor sensitivity. The measurements were performed using 5kHz resolution over a bandwidth of 50 MHz (Paper III) and 60 MHz (Paper V) with center frequencies at 825 MHz (Paper III) and 860 MHz (Paper V). However, only data within 10 MHz around the center frequency was used for the analysis, which is representative of the target LTE bandwidths for uplink and downlink channels defined in [29] to be between 1.4 MHz and 20 MHz.

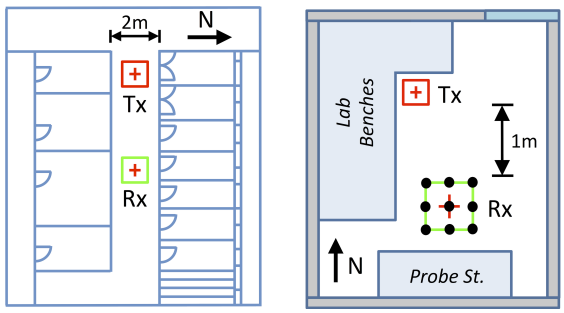

Figure 2.5: Propagation measurement setup examples - corridor (left), shielded room (right).

Figure 2.5 shows examples of the propagation measurement setup for a corridor and a shielded room environments (also discussed in Paper V). The corridor environment is located in the basement of the North-wing of the E-building at Lund University, whereas the shielded room scenario was measured in the RF-shielded room of a Lund University research laboratory. Multiple samples at different RX locations (9 for the setup in Fig. 2.5) spaced 1 λ apart were measured and used as independent channel realizations together with frequency samples spaced more than the channel coherence bandwidth apart. All realizations were averaged to ensure good fading statistics. Moreover, additional averaging was directly set in the instrument to obtain high signal-to-noise ratio. In Paper III similar setup and analysis method were used.

Chapter 3

User Interaction in Terminal Antennas

Explosive growth in the telecommunications industry over the past two decades inspired active research in terminal antenna design and optimization. Novel designs were often motivated by the challenges presented in newer communication standards targeting higher system capacity and improved reliability. This chapter briefly introduces MIMO terminal antenna requirements and design challenges before focusing in detail on a key challenge that is also one of the main topics in this thesis *i.e.*, user effects in handset antennas. Simulation and measurement models are presented, followed by illustrative examples and key findings on user effects in this thesis based on several generic terminals.

3.1 Introduction

One of the first implementations of multiple antennas in user equipment (UE) was realized in the 1990's for the Japanese Personal Digital Cellular (PDC) system when a second RX antenna was added to improve link quality [30]. Since then multiple terminal antennas were employed in various standards, including High Speed Packet Access (HSPA), as a means of higher performance. It wasn't until LTE Release 8 that it became a requirement to have two cellular antennas per frequency band in order to support MIMO operation [29]. On the other hand, standardization bodies, such as the Cellular Telecommunications Industry Association (CTIA), set further guidelines on over-the-air (OTA) operation, including various user interaction scenarios [31]. Hence, in practice mobile terminal design revolves around meeting standard specifications.

Design Requirements and Challenges

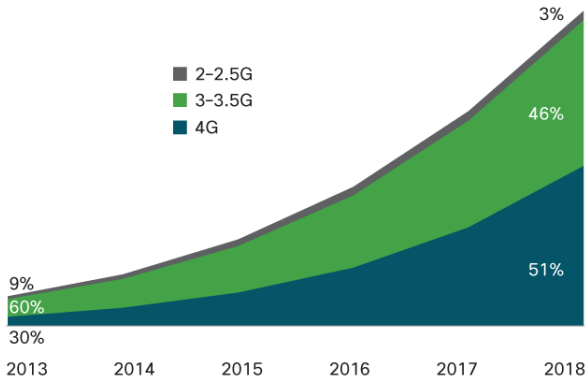

Figure 3.1: Mobile data traffic prediction [32] ©2014 Cisco.

According to [32] mobile data traffic is expected to increase 11-fold in the period 2013-2018, and worldwide LTE usage is expected to reach 51% of the total mobile data traffic in 2018 (see Fig. 3.1). In part this promising prediction depends on terminal antennas fulfilling more stringent requirements. Within the MIMO systems framework, discussed in Chapter 2, the most fundamental antenna requirements are in terms of bandwidth, efficiency, correlation and mutual coupling. Additional requirements, specific to terminal antennas, are stringent size constraints as well as efficient performance in the presence of users. Each of these requirements poses challenges to antenna and communication system designers, but some of the most relevant limitations in MIMO terminal antenna design are the compact physical size of handsets, the spatial correlation between antenna elements and the user-induced performance degradation [33]:

- **Size constraint:** An average sized handset in 2015 is confined within a $140 \times 70 \times 7$ mm^3 volume [34] where the allocated size for the antenna elements is only a small fraction of the total volume. This size constraint poses bandwidth limitations as the maximum achievable bandwidth is proportional to the radius of the sphere enclosing the antenna [35], [36].

- **Coupling and correlation:** The length of the above-mentioned volume translates to 0.37λ at 800 MHz. At such close spacing antennas suffer from high spatial correlation and electromagnetic coupling that can significantly degrade the multiplexing efficiency of the multiple antenna system. Hence, the small antenna spacing imposes a limit on the

number of antenna elements that can be implemented [33]. Currently, only two elements are required, but future releases of LTE and LTE-A specify the need of four or more elements, significantly complicating future terminal antenna design [8]. Moreover, it is known that antenna elements on a compact chassis may end up sharing the chassis for radiation, which further increases coupling and complicates efficient MIMO antenna design [37].

• **User interaction:** When in usage, the object that is commonly in the vicinity of every terminal antenna is the user hand, head or torso, depending on the user scenario. Even though it is known that antenna performance degrades in the presence of the user [33], due to absorption and mismatch losses, no unified design strategy targeting user interaction has been developed. Antenna engineers' intuition and experience still define user robust terminal antenna designs. In practice, standardization of user interaction with the terminal is available to some extent in the CTIA guidelines for handset over-the-air (OTA) performance [31]. However, changes in the phone form factor and variations between users result in new usage scenarios further increasing terminal design complexity, highlighting the need for a common user-robust terminal design strategy.

User Induced Degradation

The introduction of second-generation cellular communications in the early 1990s triggered an increasing number of research activities on the effects of users on mobile phone performance. The two main aspects investigated were 1) health hazard issues and 2) antenna performance degradation. As the first aspect is outside the scope of this work, in the following paragraphs we will focus our attention on some of the fundamental research work carried out on the second aspect *i.e.*, user induced performance degradation.

Two pioneering contributions in [38] and [39] employed custom-developed finite-difference time-domain (FDTD) simulation software to investigate antenna performance in the presence of users. In [38] the operator's (user's) influence on radiation pattern, input impedance, radiation efficiency, and near-field magnitude has been investigated. It was established that when an antenna is used by an operator the resonance frequency drops, the radiation pattern changes significantly, and on average 45% of the power is lost in the hand and head. In [39], the need for integrated terminal antenna solutions motivated the authors to investigate and compare the performance of several different antenna types in the presence of head and hand. The study outlined a noticeable effect of the user on antenna input impedance, radiation pattern and gain for

both internal and external configurations. In particular, it was shown that the planar inverted-F antenna (PIFA) was more susceptible to user interaction as compared to a standard monopole antenna. Moreover, specific absorption rate (SAR) was investigated. It was established that antenna location with respect to the user has a significant impact not only on SAR but also on mismatch losses caused by the user.

Later contributions in [40] and [41] investigated in detail the effects of real test subjects on handheld terminal antennas. The study in [40] measured received signal power and established user induced losses of up to 10 dB for different antenna types. Moreover, peak variations among users of more than 10 dB were recorded. In [41] 44 test subjects were measured in an anechoic chamber and a total body loss between 0.9 dB and 16 dB was recorded. Furthermore, absorption and mismatch contributions were separated. It was concluded that the absorption loss dominates, whereas mismatch losses contribute with up to 2 dB to the total body loss.

Figure 3.2: IndexSAR CTIA hand phantom [46].

More recent contributions, [42–45], and references therein, focus on more contemporary terminal antennas and user scenarios. Antenna impedance variations due to user proximity and mobile phone grip style variations were investigated. The study in [42] established a sharp increase in the level of impedance mismatch when part of the hand or fingers are located directly above the antenna. Impedance mismatch with voltage standing wave ratio (VSWR) of above 5 was observed. In [43] even more severe user-induced degradations were recorded for a slot antenna. Maximum radiated power of -20.5 dB was measured for the antenna in the presence of a user phantom referenced to a free

space scenario. However, the severe loss was attributed not only to absorption and mismatch but also to antenna feed disruption. Later in [44] MIMO channel capacity was examined for a coupling element-based multi-antenna structure. Capacity reductions of up to 3.6 bits/s/Hz were measured in an outdoor environment. It was also concluded that user effects are much more severe when all multi-antenna elements are in close proximity to the user. In [45] a grip study for a sample population of 100 subjects was performed aiming to explore user effects and outline in detail the typical finger and hand positions for talk and data modes.

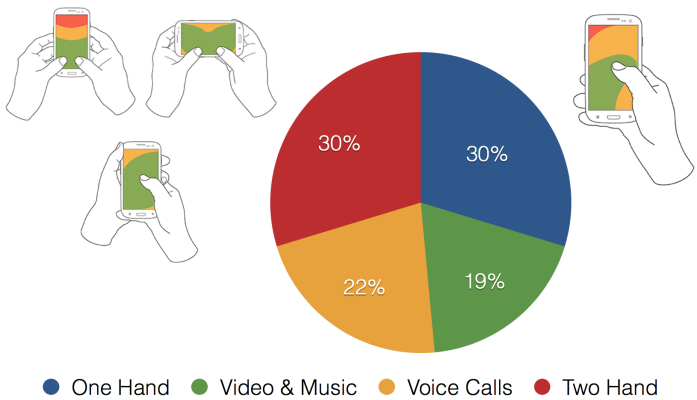

Figure 3.3: Smartphone usage [48].

Even though the contributions discussed above paved the way for future work and discussed most of the challenges users pose on terminal antenna performance, different user setups were employed producing results that are not easily repeatable. Developing standard user models is a challenging task. Even when successful, the resultant models have a limited ability to represent the wide variation in human anatomy. However, in order to have a common reference and highly repeatable results for terminal antenna performance in presence of users, standard hand and head phantoms were developed. An indexSAR CTIA standardized hand phantom [46] is shown in Fig. 3.2. Other phantom models targeting various grip styles, including use of tablets and wider smartphones, have been developed and are available from SPEAG [47]. Nevertheless, for a recent study in [48] the author observed 1333 people using mobile devices and concluded that with the evolving smartphone size and application people use devices in novel ways, such as a two hand cradle mode and a two hand portrait browse mode. Figure 3.3 shows these novel user scenarios and

outlines the one hand and several different two hand scenarios as the most common, accounting for 60% of all observed smartphone usage.

In conclusion, all studies summarized above outline several key ideas on user interaction in mobile handsets. First and foremost, users significantly degrade terminal performance by detuning antennas from their initial resonance frequencies and by absorbing a significant portion of the radiated power, thus severely reducing SNR. Secondly, it is very challenging to accurately predict the extent of user induced degradation due to the evolving smartphone size and antenna design as well as the inherent human anatomy variations and ever changing usage scenarios.

3.2 Simulation and Measurement Setup

Throughout this thesis work various user scenarios and terminal antenna types have been studied. This section presents some of the simulation and experimental user models employed.

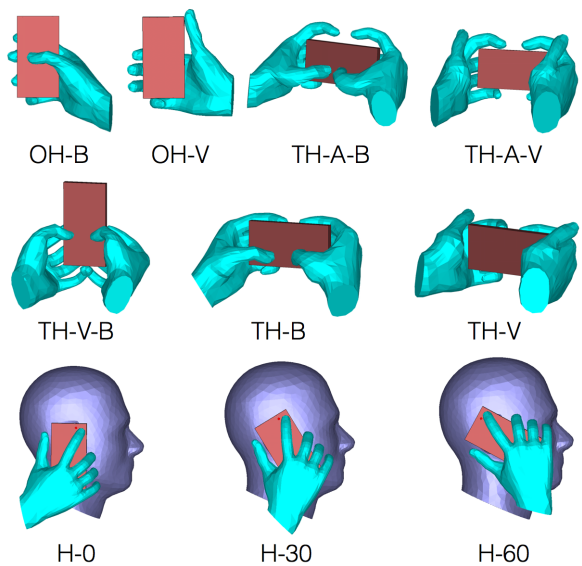

Figure 3.4: User scenario simulation setups [49]. Talk modes with different inclination angle (H-0, H-30, and H-60). Browse modes in both one and two hands (OH-B, TH-B, TH-A-B, and TH-V-B). Video modes in both one and two hands (OH-V, TH-V, and TH-A-V).

Simulation User Setups

In response to the increasing number of hand grips discussed in Section 3.1, both CTIA standardized grips and custom designed grips have been investigated in simulations. The custom grips have been designed using the same tissue composition and relative size of the CTIA standardized hand [31], whereas the position of the fingers and palm as well as their orientation with respect to the terminal have been adjusted according to novel grip styles. Initially, three custom grips were designed and simulated in [17] (Paper II). Later in [49] (Paper I) a total of 10 user scenarios were developed and investigated - 2 one hand (OH), 5 two hand (TH) and 3 talk (H) modes. The exact position and orientation of the hand and head for the custom designed user scenarios are shown in detail in Fig. 3.4.

Experimental User Setups

Figure 3.5: Phantom user scenario setups. Propagation measurement in a TH mode with head and torso in an outdoor environment [50] (left). Radiation pattern measurement in a TH mode with phantom hands only [18] (right) ©2013 IEEE.

The experimental studies carried out during this thesis work focused on propagation channel measurements and antenna radiation pattern measurements. Both were executed with and without users present, either as phantoms or as real test subjects. Figure 3.5 shows the setups for propagation and pattern measurements with CTIA standardized phantom hands from indexSAR [46] and a torso phantom. In addition to the TH user scenarios shown in Fig. 3.5, OH scenarios were also experimentally studied in [18], [50], and [51] (Papers III-V).

In order to address concerns expressed in [52] and [53] that human phantoms underestimate user induced degradations as compared to real test sub-

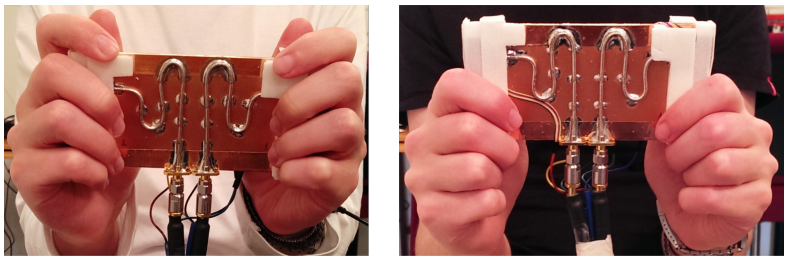

Figure 3.6: Real test subject measurement setups - firm grip (left) and freestyle grip (right).

jects, channel measurements with 10 test subjects in different handgrips and propagation environments were performed in [51] (Paper V). The 10 users were of both genders mainly from Europe but also from Asia, Middle East and North America. Users were asked to reproduce a firm grip and a freestyle grip shown in Fig. 3.6. The firm grip covered a larger portion of the terminal's short edges as compared to the freestyle grip.

3.3 Results and Discussion

Simulated results on the user effects of two MIMO dual-band antenna prototypes will be presented in this section to demonstrate a few fundamental principles of user-induced terminal degradations. The specifications of the terminals are briefly discussed below followed by results and discussions on some of the simulation and experimental studies performed during this thesis work.

IFA: The IFA prototype from [49] (Paper I) is similar in design to the one used in [54] with a volume of $130 \times 66 \times 7\text{mm}^2$. It comprises two identical dual-band IFAs located on the opposite short edges of the chassis, targeting LTE Band 5 (824-894 MHz) and LTE Band 2 (1.85-1.99 GHz). The simulated prototype efficiency, mutual coupling, and envelope correlation in free space (FS) at $f = 860$ MHz are: $\eta_{1,2} = -3.3$ dB, $S_{21} = -4.1$ dB, $\rho_e = 0.4$.

PIFA-Monopole: The PIFA-Monopole prototype from [49] (Paper I) is also a dual-band terminal, but consisting of a PIFA element and a folded monopole element. It is identical in size to the IFA prototype and targets the same frequency bands. However, the limited bandwidth of the PIFA in the low band limits the terminal bandwidth in LTE Band 5 to 31 MHz, sufficient to cover only the downlink (adequate for LTE, which uses MIMO only on the downlink). The simulated prototype efficiency, mutual coupling, and envelope correlation

in the low band in FS are: $\eta_{\text{PIFA}} = -2.5$ dB, $\eta_{\text{mono}} = -2.4$ dB, $S_{21} = -7.8$ dB, $\rho_{\text{e}} = 0.5$. In [17] (Paper II) different PIFA-Monopole prototypes were used, where the main difference was the monopole element (slot monopole instead of a folded monopole).

Simulation Studies

In mobile communications the terminal is required to operate efficiently in any orientation motivating the general requirement on terminal antennas to be omnidirectional. This can be seen in Fig. 3.7, where the electric far-field radiation pattern of the IFA prototype, described earlier, is presented with and without a user hand present (*i.e.*, OH-B scenario). In FS the handset exhibits a rather omnidirectional pattern as expected. However, in the OH-B user scenario the hand significantly reshaped the radiation pattern focusing the direction of maximum radiation away from the hand. Moreover, looking at the intensity, we notice that the electric field magnitude was reduced unevenly in the angular domain due to the presence of the hand. This is an indication of one of the key user effects in terminals *i.e.*, absorption loss. A significant portion of the radiated power is absorbed in the hand and therefore lost.

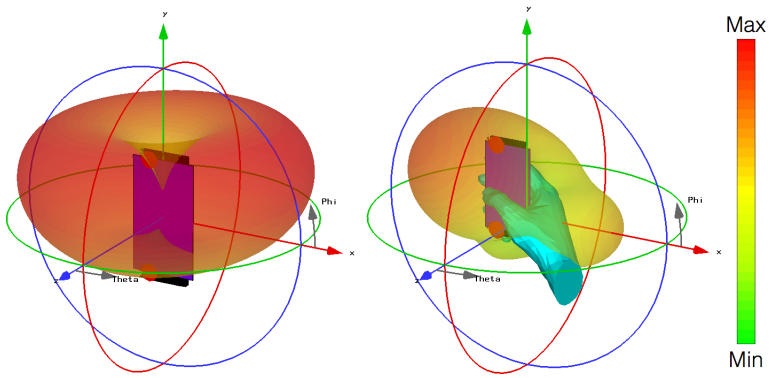

Figure 3.7: IFA prototype electric far-field radiation pattern - FS (left) and OH-B (right), both at $f = 860$MHz.

In order to quantify absorption loss we study how the antenna radiation efficiency changes with respect to the FS case. This method is applicable given that the losses in the metal and dielectric of the terminal are notably smaller as compared to user-induced absorption. The results presented in Fig. 3.8 were obtained according to the discussion above, by averaging over the frequency band of operation (LTE Band 5). As intuition would suggest the head (with

hand) cases suffer from highest absorption losses (up to 10.4 dB for IFA in H-30). Fortunately, the talk modes do not have as high data rate requirements as the rest of the cases, since during a voice call (with the terminal held next to the head) the most data rate demanding tasks such as browsing and video streaming are not applicable. For the remaining scenarios in Fig. 3.8, the absorption loss is between 2.3 dB for PIFA-Monopole in OH-B and 4.2 dB for IFA in TH-B which is consistent with the observations in [38] and [39].

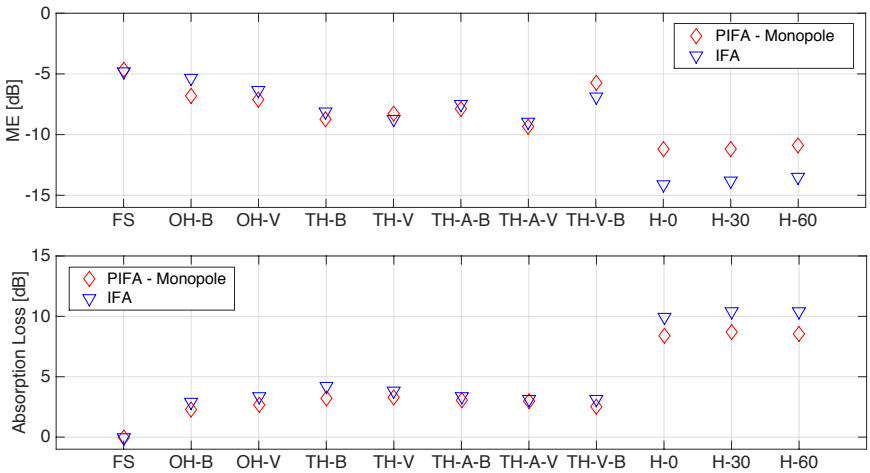

Figure 3.8: Multiplexing efficiency and absorption loss for two prototypes in 11 cases averaged over LTE Band 5.

Nevertheless, absorption loss does not fully describe user interaction in terminals. The antenna matching and coupling efficiency (*i.e.*, at port 1 $\eta_{\mathrm{M}} = 1 - |S_{11}|^2 - |S_{21}|^2$), as well as the envelope correlation, have a significant impact on MIMO handset performance. Figure 3.8 presents the ME for all cases and both prototypes. As discussed in Chapter 2, ME combines antenna total efficiency (accounting for radiation, mismatch and coupling) and correlation to give a system level estimation of the terminal performance. It is interesting to note that the relatively large absorption losses discussed earlier do not necessarily translate to the ME shown in Fig. 3.8, emphasizing the important interplay between efficiency terms and correlation. The performance of the IFA prototype in OH-B is a good example, where the ME drops by only 0.5 dB as compared to FS, even though there is an absorption loss of 2.9 dB. This is due to the presence of the hand which reduced the correlation (from 0.4 to 0.1) and mutual coupling (from -4.1 dB to -7.8 dB), therefore counteracting

part of the absorption losses. Nevertheless, this reasoning is specific to the IFA prototype in the OH-B mode. In other cases such as the TH-V mode the absorption loss of 3.8 dB translates more directly to the ME loss of 3.9 dB as compared to FS. In this case the correlation was not significantly affected by the hands, whereas the mismatch efficiency also did not change significantly (-2.8 dB in FS vs. -2.6 dB in TH-V), since the reduced coupling due to the hands is counteracted by the antenna resonance offset (indicated by $|S_{11}|$ and $|S_{22}|$). In general, the effect of users on terminal antenna correlation is hard to predict as it is dependent on the exact position of the hand and head and is very specific to individual grip styles and users. Overall, the above discussion emphasizes that terminal performance in the presence of users is the result of a complex interplay between efficiency, correlation, coupling and absorption losses.

Another very important factor to be considered when studying user effects in terminals is antenna bandwidth. In [17] (Paper II) and [18] (Paper IV), terminals with different bandwidth were investigated. It was established that the wider the bandwidth of the terminal the more resilient it is to user interaction. This conclusion is very intuitive since narrowband antennas are much more prone to mismatch (resonance frequency offset) due to their limited bandwidth potential. Unfortunately, wide band terminal designs are difficult to achieve and often sacrifices are made in correlation or antenna efficiency as seen in [18] (Paper IV). Therefore, other methods for user resilient terminal design can also be explored, such as antenna switching or EM shielding.

Experimental Studies

Experimental verification of user interaction was performed in [18] (Paper IV) with phantom hands and in [50] (Paper III) with phantom hands and torso. Anechoic chamber measurements of the IFA prototype in TH and OH modes showed ME of -9.9 dB and -6.1 dB respectively, which are consistent with the simulated results in Fig 3.8. The propagation measurements in [50] (Paper III) with head and torso were discussed in terms of MIMO capacity. It was concluded that the TH grip leads to a 36 % drop in capacity as compared to FS, further demonstrating severe user induced degradations in an experimental setup.

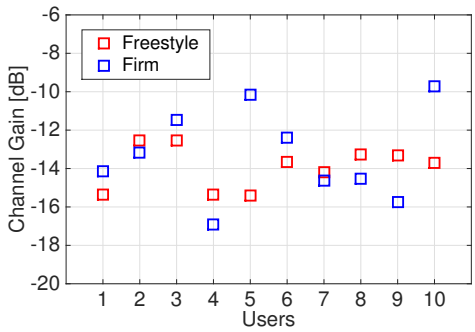

Figure 3.9: Measured channel gain in a shielded room environment.

Moreover, in [51] (Paper V) both phantoms and real test subjects were experimentally investigated. Figure 3.9 shows the measured channel gain for the real users in two handgrips referenced to FS. In the firm grip channel gains from -10 dB to -17 dB were measured over different users, whereas in the freestyle grip smaller variations over users were observed (from -12.5 dB to -15.4 dB). This result is expected as in the freestyle grip less terminal antenna area is covered by the hands and therefore any variations in hand size and location have a smaller impact on performance. Nevertheless, the measured channel gain variations over users are significant and indicate how the wide variety of user hand size can influence performance, as was established in some of the early publications in the field [40, 41]. Moreover, in [51] (Paper V) the terminal performance with real users was compared to that with the indexSAR phantom hands. It was suggested that on average real users exhibit 2 dB higher mismatch losses as compared to the phantoms. Furthermore, high absorption losses (over 6 dB in the freestyle grip) were measured. In comparison, the absorption losses in Fig. 3.8 are less than 5 dB in all hand cases. This further supports the initial results in [52] and [53] suggesting that phantoms have the tendency to underestimate user interaction effects.

Chapter 4

User Resilient Terminal Design

Previous discussions in this work pointed out that terminal antenna design is subject to many constraints and challenges. However, despite the restrictions in terms of size and performance, significant advances in terminal antenna design have been made in the past decade. This chapter investigates several terminal antenna prototypes, including conventional designs and some more recent designs. The aim is to evaluate their effectiveness under user influence and draw conclusions on user robust designs. In the first part of the chapter several contributions on handset antenna performance in the presence of users are discussed. Next, the simulation study on user effects of five state-of-the-art dual-antenna terminal designs is described. The chapter concludes with results and discussions on the performance of the investigated terminals.

4.1 Introduction

Even though handset antenna design is limited by the volume provided in a mobile terminal, efficient usage of this limited space can provide improved performance in the presence of users. The ultimate goal is to minimize absorption by the hand and head of users while efficiently transferring power from the RF front-end to the antenna elements. Research contributions over the past two decades have examined user effect variations with antenna type. In [39] a monopole and several different PIFAs were investigated as potential candidates for integrated handset antennas. It was established that the PIFAs are more susceptible to user induced mismatch losses. Later, in [41], comprehensive mea-

surements with 44 test subjects have shown that the patch antenna investigated in the study exhibits 6 dB lower absorption loss compared to a helix antenna. Recent contributions targeting LTE have proposed different strategies for improving antenna performance in the presence of users. In [55], the authors studied user effects for capacitive coupling element (CCE) based antennas. It was observed that the shape, size and location of the CCE elements significantly affect antenna performance, concluding that a multi-element structure with antenna switching is beneficial in the user scenarios studied. Moreover, this study emphasized the need for detailed tests in more measurement grips including talk modes with the head phantom present. Later in [56] an antenna shielding approach was used to reduce user effects based on the idea presented in [55]. By switching between two co-located CCE elements total efficiency improvements of up to 5 dB were recorded. Another approach is to add parasitic antenna elements in order to reduce absorption and mismatch losses. The study in [57] utilized a Z element and showed a total loss reduction of 2.3 dB. Later in [58] the effect of the index finger position on a narrow bandwidth prototype and a wide bandwidth prototype was studied. It was observed that the narrow bandwidth prototype suffered lower user induced losses in both top and bottom element mounting positions on the chassis. Moreover, this contribution also identified the need for more comprehensive user effect studies in various hand grips and user cases.

More recently, the Theory of Characteristic Modes (TCM) [59] was successfully applied to design efficient MIMO terminals. The study in [60] showed a three-port MIMO handset antenna design at 2.5 GHz, where the terminal efficiently excited three characteristic modes to achieve high antenna efficiency and low envelope correlation. To address the challenging problem of designing MIMO terminal antennas for frequencies below 1 GHz, a MIMO antenna system based on realistic form factor and packaging implementation was presented in [61]. TCM analysis of ground plane modifications has been applied to achieve high isolation and low correlation at 750 MHz. In [37] a monopole and a T-strip structure were used to excite orthogonal modes for a MIMO terminal targeting a LTE band below 1 GHz. Moreover, this contribution presented a user effect study based on two user scenarios. Later in [62] the authors extended the work from [37] to achieve an efficient dual-band design by using correlation of currents and near-fields of characteristic modes across frequencies. Moreover, in [63] a bezel structure was employed using TCM to provide another dual-band MIMO antenna design with excellent performance in the low frequency band and acceptable efficiency and correlation in the high frequency band. Nevertheless, even though the contributions in [37, 60–63] revealed innovative terminal antenna designs, only the study in [37] verified the antenna performance in the presence of users. However, only two data mode user sce-

narios were investigated, which points to the need for a more comprehensive study on the user effects in TCM-based terminals.

4.2 MIMO Prototypes

During this thesis work, the performance of several MIMO terminal prototypes has been investigated in the presence of users. The study in [50] (Paper I) looked into five representative designs including conventional antenna types and geometries as well as more recent designs based on TCM. Figure 4.1 shows all five MIMO prototypes as well as the feeding locations and port numbering. The target operating frequencies for all terminals were LTE Band 5 (824-894 MHz) and LTE Band 2 (1850-1990 MHz). Prototypes 1 and 2 were proposed in [62] and [63], respectively, and were designed based on TCM. Prototypes 3, 4 and 5 include more conventional antenna types (PIFA, monopole etc.) and have been presented in [18], [64] and [54], respectively. More studies beyond the investigation in [49] (Paper I) have been done in Papers II-V. For example Prototype 5 was used in the propagation channel measurements in [50] (Paper III) and [51] (Paper V), whereas Prototypes 3 and 5 have been measured in a SATIMO Stargate measurement system [65] in both a OH and a TH user grip for the study in [18] (Paper IV).

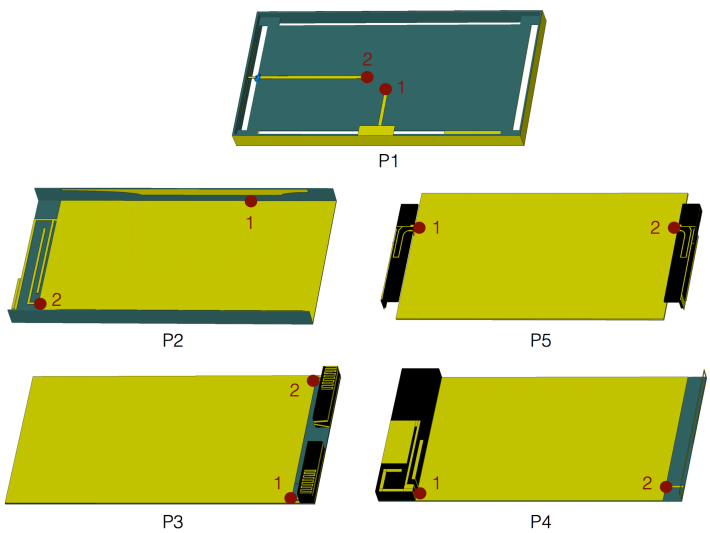

Figure 4.1: MIMO terminal prototypes investigated in [49] (Paper I).

In terms of the free-space performance in the low frequency band, Prototypes 1 and 2 showed very good efficiency, isolation and correlation, whereas Prototype 3 had the largest bandwidth. Prototypes 4 and 5, on the other hand, are more conventional structures and were outperformed by the other terminals in terms of bandwidth (by Prototype 3) and in terms of efficiency and correlation (by Prototypes 1 and 2). The advantages of Prototypes 1 and 2 are due to the design strategy used. Specifically, TCM was employed to efficiently excite different characteristic modes resulting in orthogonal radiation patterns, giving the low correlation and high isolation mentioned above. However, the question on whether the free-space performance of these prototypes is preserved in the presence of users still remains open.

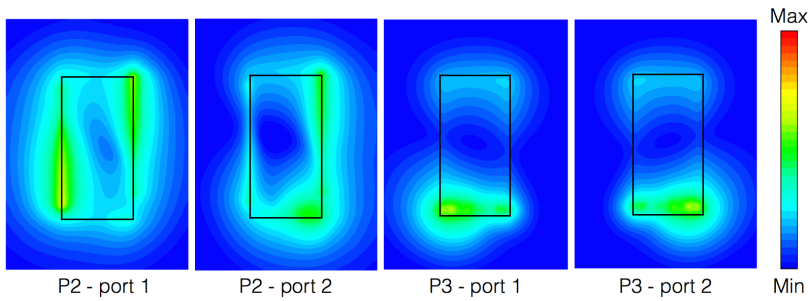

Figure 4.2: Electric field magnitude for a reference plane 10 mm above the terminal ground plane in the FS scenario.

In Section 3.3 of this thesis user interaction was demonstrated for an IFA-based terminal (*i.e.*, Prototype 5) and a PIFA-Monopole terminal (*i.e.*, Prototype 4) emphasizing key aspects such as absorption, mismatch, bandwidth and the important interplay between efficiency, coupling and correlation. However, the discussion had thus far omitted another important factor, namely near-field distribution. Due to the small spacing to the handset users are in the near-field of terminal antennas. It is therefore crucial to consider near-field distribution when identifying the main causes of user induced degradation. In this context another interesting difference between the TCM-based designs and the more conventional designs was observed. Due to the efficient utilization of the ground plane, the TCM-based designs exhibit more spread near-field distribution as compared to the more localized distribution recorded for the conventional terminals. To demonstrate this difference the electric field magnitude is plotted in Fig. 4.2 for a plane 10 mm above the terminal ground plane. It can be seen from the results that Prototype 3 shows more localized radiation as compared to Prototype 2 in the FS scenario. Similar conclusions were drawn for

P1 and P4. In the following subsection the consequences of such near-field characteristics will be discussed in the context of user interaction.

4.3 Results and Discussion

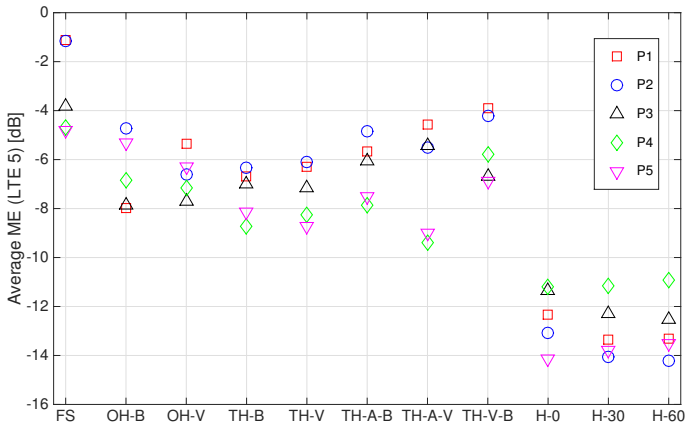

Figure 4.3: Average ME over LTE Band 5.

The average performance of all five terminals is shown in Fig. 4.3 for the user scenarios presented in Fig. 3.4. Aside from the ME advantage in FS, Prototypes 1 and 2 also show better performance than Prototypes 3-5 in most of the data mode user cases. The detailed investigation in [49] (Paper I) attributed these differences to a consistently low envelope correlation as well as high matching and coupling efficiency of both Prototypes 1 and 2. Nevertheless, it was also concluded that TCM-based designs suffer from higher absorption losses. This result strongly relates to the near-field discussion presented above. In general the closer the user is to the regions of high near-fields the larger the absorption loss. As the near-field hot spots for Prototype 1 and 2 are spread out through the entire terminal, the probability that the user hand will be close to one of them is higher than for the terminals with more localized near-field distribution leading to lower absorption losses for Prototypes 3-5. This argument was extended in [49] (Paper I) where specific user cases were discussed in terms of the relative position of the hand with respect to the near-field hot spots. Overall, the effect of the higher absorption losses was smaller than the gains due to the lower correlation and better impedance matching, leading to

the better performance of Prototype 1 and 2 in the data modes. However, in the talk modes (H-0, H-30, and H-60) the correlation advantage of Prototype 1 and 2 was not present due to asymmetric scattering from the head resulting in low correlation for all terminals. Hence, Prototypes 1 and 2 were outperformed by some of the conventional designs.

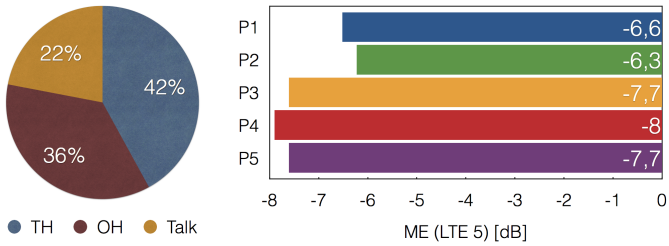

Figure 4.4: Weighted terminal usage over LTE Band 5.

Nevertheless, in practice different user hand grips have different impact on overall performance, since some grips are used more often than others. However, estimating the usage distribution of different grip styles is very challenging due to the large number of observations needed to produce statistically relevant results. Moreover, with smartphone size evolving rapidly any conclusions based on such a study would be specific to certain form factors. These challenges partly explain the lack of studies done on determining the usage distribution of hand grips in practice. Fortunately, the study in [48] provided some initial results based on real-world observations of 1333 people using smartphones. The devices observed have a similar form factor to the terminals investigated in this thesis (length 130-140 mm and width 65-70 mm). Therefore, inspired by the results in [48], this thesis proposes the smartphone usage distribution shown in Fig. 4.4. In [49] (Paper I) the user scenarios from Fig. 3.4 were mapped to the proposed distribution in order to evaluate the overall usage-weighted terminal performance. As seen in Fig. 4.4 the TCM-based prototypes show weighted MEs that are 1.1-1.7 dB higher than the conventional designs, confirming the initial observations from Fig. 4.3 in a more practical context. Based on this overall performance it can be concluded that TCM is a promising strategy for designing efficient terminal antennas in the presence of users.

In conclusion, this chapter summarized some existing work on mitigating user effects using antenna design. Moreover, it also presented the major findings from an user effect mitigation through antenna design, involving the evaluation of 5 terminal antennas in a variety of user scenarios. It was found that significant improvements are feasible with a new design strategy based on TCM, where usage-weighted performance gains of up to 1.7 dB have been achieved.

Chapter 5

Adaptive Impedance Matching

Aside from user-robust antenna designs, another approach to user effect mitigation is to add passive circuit components in order to match the antenna impedance to the input impedance of the RF front end module which increases antenna efficiency. In general this approach is broadly known as impedance matching, or adaptive impedance matching (AIM) when the system includes components with variable impedances and is able to detect time-varying mismatch and react to it. This chapter discusses the potential of AIM to improve antenna and system performance in the presence of users. First, a general introduction of AIM is presented including concept, key technologies and current designs. Then the simulation and measurement setups are discussed followed by both simulation and experimental results. Finally, a technology demonstrator developed as part of this thesis work is described. The demonstrator is capable of displaying near real-time user effect mitigation.

5.1 Introduction

Optimizing antenna performance with impedance matching networks has been around for decades [9]. However, over the past years several key contributions have extended the knowledge on the subject with both theoretical derivations and experimental verifications. Two of the fundamental studies in the field use a rigorous network theory approach to examine multiport matching networks [66, 67]. In [66] coupled dipole antennas were analyzed to demonstrate the diversity performance for different terminations provided by matching networks, whereas

in [67] a framework for the analysis of mutual coupling is presented focusing on the capacity of MIMO systems with different impedance matching conditions. Later in [68] uncoupled matching networks were used to realize a 2.8 dB power gain for a closely coupled two-dipole array at the expense of a higher envelope correlation, pointing out an interesting tradeoff between maximum received power and minimum correlation. The follow-up work in [69] derived a closed form expression of the optimum impedance matching for maximum capacity. Subsequent studies in [70–72] proposed and verified a very practical method for investigating the effects of variable impedance matching on multiple antenna systems. Results from full-wave and circuit simulations were combined in order to save computational time and predict effective antenna parameters without having to run detailed simulations for all impedance conditions investigated. In [70] and [71] the method was described in detail, whereas [72] focused on MIMO capacity optimization using the method. A few other studies take into account different propagation environments. In [73] different capacity gains from impedance matching were observed over different environments (uniform 2D APS vs. Laplacian 2D APS). Furthermore, in [74] active matching has been shown to be more effective than passive matching in cases with high mutual coupling or low SNR over various propagation environments. More recently, in [75], a random search algorithm was applied to uncoupled matching networks to optimize the capacity of channels with different angular spreads (ASs). Nevertheless, none of the studies above tackle explicitly user interaction, nor do they investigate realistic impedance tuners.

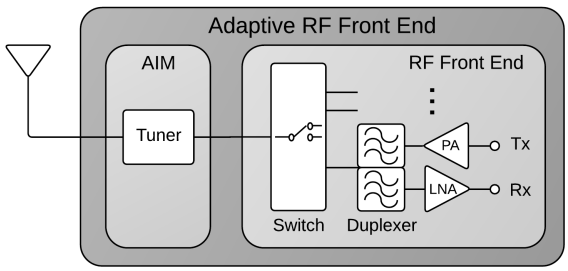

Figure 5.1: Adaptive RF front end setup.

In practice terminal antenna AIM is typically realized as a separate circuit module that sits between the RF front end and the antenna (see Fig. 5.1). This placement is very practical for antenna tuning but very demanding from a circuit design perspective. The module needs to operate over a wide band-

width, handle both TX and RX power levels, and add minimal losses to the system. In practice closed loop and open loop solutions exist, whereas only the closed loop solution can handle both static (amplifier-antenna) and dynamic (user induced) mismatches [53]. In this work closed loop tuners were investigated targeting user interaction in particular. The tuning components were realized analytically and experimentally, whereas the optimum impedance state selection was done with MATLAB [76] and LabVIEW [77].

Key Technologies

The key components of most state-of-the-art AIM tuners are digitally tunable capacitors (DTC). Typically one or more DTCs are combined with off-chip or on-chip inductors to form standard LC or more complicated π and double π variable impedance matching networks. Off-the-shelf DTCs are fabricated in different processes exhibiting performance tradeoffs depending on the technology used. Some of the most common processes used in DTC manufacturing are shown in Fig. 5.2. These include complementary metal-oxide-semiconductor (CMOS), micro-electro-mechanical-systems (MEMS), III/V semiconductor and barium strontium titanate (BST) based semiconductor. Capacitors manufactured in these processes are available from a wide variety of suppliers including EPCOS TDK, WiSpry Inc., STMicroelectronics, Peregrine Semiconductor, and BlackBerry Limited.

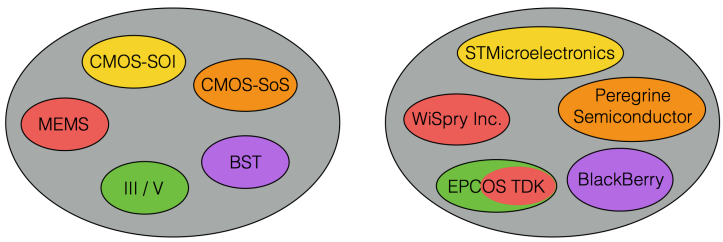

Figure 5.2: Antenna tuner manufacturing technologies (left) color coded to the respective suppliers (right).

A summary of the performance tradeoffs between different processes is presented in Fig. 5.3 based on [78]. The comparison is done both in terms of performance related and implementation related figures of merit (FOMs). Important FOMs for RF performance are induced losses, DTC range, bias voltage levels and power handling capabilities. Moreover, reliability, cost and package size need to be strongly considered as the target products *i.e.*, smartphones, are produced in volumes of hundred of millions per year and have very lim-

	Parameters	Silicon		III/V	MEMS	BST
		CMOS SOI	CMOS			
Figures of Merit	Range	Wide	Medium	Wide	Wide	Narrow
	Losses	✓	✓	✓✓	✓✓✓	✓✓✓
	Bias Voltage	✓✓	✓✓	✓	XX	XX
	Power Handling	✓	XX	✓	✓✓✓	✓✓
Implementation	Reliability	✓✓	✓✓	✓✓	X	NA
	Cost	✓✓	✓✓	✓	X	XX
	Size	Small	Small	Small	Big	Big

Figure 5.3: Comparison of different tuner technologies [78].

ited space for additional circuit modules. In terms of RF performance MEMS is the process that can offer lower losses, higher linearity and higher power handling compared to the other technologies. Nevertheless, MEMS exhibits key disadvantages related to implementation such as higher cost, higher process complexity, bigger packaging and questionable reliability. These drawbacks have made it difficult for MEMS to penetrate the market on a larger scale [78, 79]. On the other hand, CMOS technology is mature and optimized for large volume productions that is also cost effective and reliable. The main tradeoff in CMOS is the inferior RF performance to MEMS. However, a new CMOS silicon on insulator (SOI) process *i.e.*, CMOS-SOI, offers significant performance advantages over standard CMOS technology. These include lower parasitic capacitance, higher performance at equivalent bias voltages and better wafer utilization. Hence, CMOS-SOI is generally considered a good compromise between RF performance, cost, package size and reliability of DTCs [78]. Therefore, CMOS-SOI was the process chosen for the tuner design in this work.

Current AIM Designs

Over the past few years a number of scientific contributions have proposed complete impedance tuner solutions targeting terminal antennas. In [80] a 0.35μm CMOS impedance tuning unit with 6 switched capacitors and 64 different matching combinations has been designed. It was established that the tuner can correct mismatches of up to VSWR=8. Yet, the loss of each module was as high as 2.1 dB. Later in [81] the authors presented a low loss RF-MEMS design of an adaptive LC matching network. High impedance correction ca-

pabilities were demonstrated for a single PIFA antenna element. Moreover, losses in the tuning module of up to 0.5 dB in both the low and high bands were measured, indicating the significant low-loss advantage of using MEMS technology as compared to standard CMOS.

More recent designs in [82] and [83] also use RF-MEMS technology. In [82] an adaptive tuning module with an insertion loss of 0.65 dB at 880 MHz was presented. It was concluded that the module can increase phone output power by 1.2 dB on average. The work in [83] also used RF-MEMS but it had more stringent insertion loss specifications: <0.3 dB (850 MHz), <0.5 dB (1800 MHz), and <0.6 dB (2100 MHz). However, the presented tuner solution struggled to perform within the specifications, especially in the higher frequency bands. The contributions in [84–86] employed a 130nm CMOS-SOI process from STMicroelectronics. In [84] and [85] a fully integrated tuner operating between 2500 MHz and 2690 MHz was presented targeting user effect compensation in 4G antennas. It was established that the tuner can successfully correct antenna mismatches of up to VSWR=5 as well as handle 30 dBm output power to satisfy LTE uplink requirements. More recently in [86] a low band (700 MHz to 900 MHz) tuner was designed in the same process (130nm CMOS-SOI). Detailed characterization of the device revealed a measured minimum loss of 1 dB, as well as high linearity and power handling capabilities. Two of these devices were implemented on the MIMO terminal measured over different user and propagation environments in [51] (Paper V).

In conclusion, impedance tuners have been analytically and empirically shown to effectively correct user induced antenna mismatches. However, the high requirements on device performance are still the main bottleneck preventing this technology from achieving significant market penetration. Nevertheless, the results in Fig. 5.3 suggest that CMOS-SOI is a promising DTC design process offering a reasonable compromise between implementation and performance.

5.2 Simulation and Measurement Setup

Throughout this project we investigated three different AIM setups - a simulation based setup with lossless tuners and two experimental setups with either automated mechanical tuners or CMOS-SOI tuner chips. During both the simulation and experimental studies, the focus was on the low band performance (below 1 GHz) since the challenges of designing MIMO terminal antennas at these frequencies are very high due to the small electrical size of the terminals [33].

Lossless Tuner Model

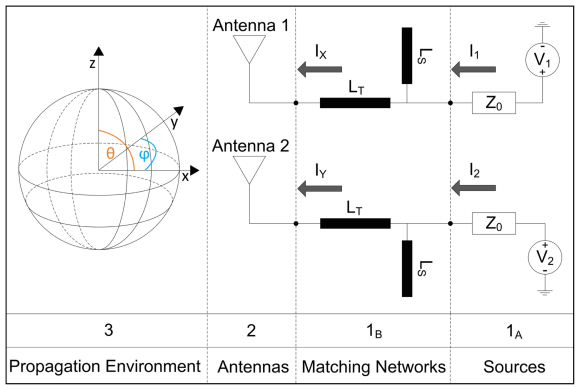

Figure 5.4: Lossless tuner model [18].

In [18] (Paper IV) the Kronecker model was used to provide the physical 2×2 MIMO channel. The receive correlation matrix was built from the RX antenna total efficiency and complex correlation coefficients, whereas the transmit correlation matrix was assumed to be equal to identity (0 correlation and 100% efficiency) since the focus in this work is to investigate downlink performance (with the terminal being the RX). The method described and verified in [70–72], was used to evaluate the antenna performance for different matching conditions. In essence, antenna embedded radiation patterns, scattering parameters and tuner states were used to evaluate the effective radiation pattern and therefore efficiency and correlation given different impedance matching states. Hence, multiple receive correlation matrices were built each describing the antenna performance in a particular impedance matching state. Moreover, non-uniform APS environments were studied using the modified MEG expres-

sion (2.16). Figure 5.4 shows the complete lossless model. The impedance matching network at each port consists of a lossless open-circuited stub and a lossless transmission line with variable length. Using this setup the entire Smith chart can be covered with a user-defined resolution. In [18] (Paper IV) 96 states were used per port (*i.e.*, a total of $96^2 = 9216$ combinations).

Automated Mechanical Tuners

In [50] (Paper III) two Maury Microwave MT982EU30 mechanical tuners [87] were directly used in the channel measurements. Propagation data was measured with a 4-port VNA according to Chapter 2.2, employing wideband monopoles at the TX and a handset prototype at the RX. The MIMO terminal used in the experiment was based on the design of Prototype 5 in [49] (Paper I) and Prototype A in [18] (Paper IV) targeting a low (800-850 MHz) and a high (2300-2400 MHz) frequency band. Tuner control was handled by a LabVIEW software, where only 10 states per port ($10^2 = 100$ combinations in total) were measured due to the slow switching speed of the tuners. Even though the Maury tuners are large and therefore impractical for terminal antenna applications, they offer a very wide and dense coverage of the Smith chart at a very low insertion loss (up to 0.4 dB at VSWR=1 according to [87]). Therefore, they were used as an intermediate step between the simulation based model and a fully integrated solution in order to verify the potential of AIM in a practical setup. Moreover, propagation results with the Maury tuners were compared to the corresponding results with lossless tuners (see Fig. 5.4) added to the measured channels in post-processing. Channel update for different impedance states was done according to the studies in [67] and [54].

Custom CMOS-SOI Tuners

During the last stage of this thesis work the custom CMOS-SOI tuner design from [86] was used in propagation channel measurements to determine the impact of a realistic impedance tuner on AIM performance. Figure 5.5 shows the circuit schematic and printed circuit board (PCB) picture of the tuner. It was designed as a double π network comprising three identical 5-bit programmable capacitors (C1, C2 and C3), and two off-chip inductors (L1=L2=7.4 nH). For the study in [51] (Paper V) two of the custom designed tuners were implemented on a prototype terminal including a battery board to ensure autonomous run of the AIM system. The propagation measurement setup used was similar to the setup during the measurements with the Maury tuners in [50] (Paper III). However, the MIMO handset (see Fig. 5.6) was retuned to target LTE Band 18 (815-875 MHz) and LTE Band 9 (1750-1880 MHz). Moreover, it included

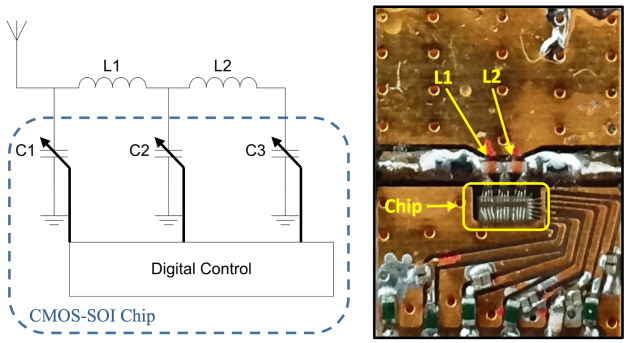

Figure 5.5: CMOS-SOI tuner circuit schematic (left) and PCB with chip and decoupling networks (right) [51].

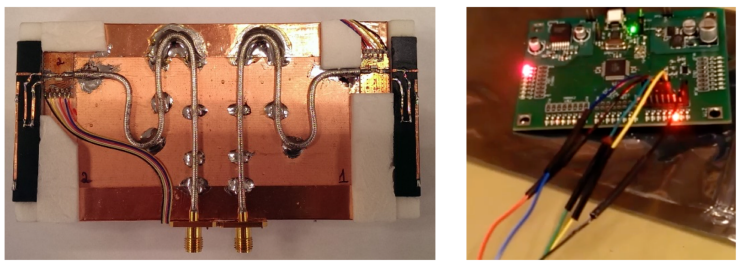

Figure 5.6: Handset prototype with CMOS-SOI impedance tuners (left) and digital control board (right).

external PCBs used to accommodate the tuner chips (see Fig. 5.5). Tuner control was done with a custom designed board (see Fig. 5.6) featuring the Atmel ATmega32 microcontroller [88]. The automation of the entire measurement system as well as near real-time data evaluation was done by a custom LabVIEW [77] software, which was responsible for communicating the required impedance states to the microprocessor via an UART interface. However, prior to running the LabVIEW software lookup tables have to be set up in the digital control board microprocessor matching specific UART commands to bit sequences for each individual state of the impedance tuner. For this reason a custom C program was developed on the ATmega 32 microcontroller in order to handle the interface between the tuners and the LabVIEW software.

5.3 Adaptive Impedance Matching Studies

In the following discussion some representative results from [17] (Paper II), [50] (Paper III), [18] (Paper IV) and [51] (Paper V) will be presented. AIM gain is shown in terms of capacity or ME as compared to the cases where no tuners were used or the tuners were set to the 50 Ω state. The optimal state is chosen from exhaustive simulations or measurements over the Smith Chart domain for the respective setups.

Simulation Studies

In [18] (Paper IV) two fundamentally different terminal designs were investigated. Prototype A is better matched ($S_{11} = -16$ dB vs. $S_{11} = -6.5$ dB) in FS, has higher mutual coupling (-5.3 dB vs. -6.3 dB) and lower bandwidth (85 MHz vs. 200 MHz) as compared to Prototype B. Employing lossless tuners to measured antenna parameters in OH and TH scenarios led to improvements in capacity and ME for both prototypes. Capacity gains of up to 43 % (4.8 dB ME gain) for Prototype A and up to 10 % (1.7 dB ME gain) for Prototype B were recorded emphasizing the significant effect of antenna design on AIM performance. This difference was attributed to the terminal bandwidth. The significantly larger bandwidth of Prototype B prevented severe resonance frequency offset and therefore resulted in smaller mismatch (hence smaller AIM gain) as compared to Prototype A.

The AIM gains observed above were mainly attributed to antenna efficiency improvements in both prototypes. However, it was also established that uncoupled matching networks can affect envelope correlation (*e.g.*, from 0.4 to 0.2 in Prototype A - TH). This effect is crucial for MIMO implementations but it is also limited in the case of uncoupled AIM to terminals with high mutual coupling. In such cases the non-excited antenna element acts as a reactively loaded parasitic element affecting the radiation patterns to reduce the envelope correlation. Therefore, the results in [18] (Paper IV) have shown that AIM has the potential to mitigate user interactions through two main mechanisms: (1) mismatch compensation to counteract efficiency degradation and (2) improvement in envelope correlation.

Extending on the significance of bandwidth in AIM studies, [17] (Paper II) presents capacity performance over the complete LTE Band 13 (746 - 787 MHz) for three different prototypes (P1-P3). Figure 5.7 shows the capacity for the optimal and the 50 Ω states in the three prototypes with identical antenna types. However, the different antenna locations on the chassis led to differences in bandwidth and isolation. The capacity performance over the system bandwidth shows that at some frequency points the 50 Ω state outper-

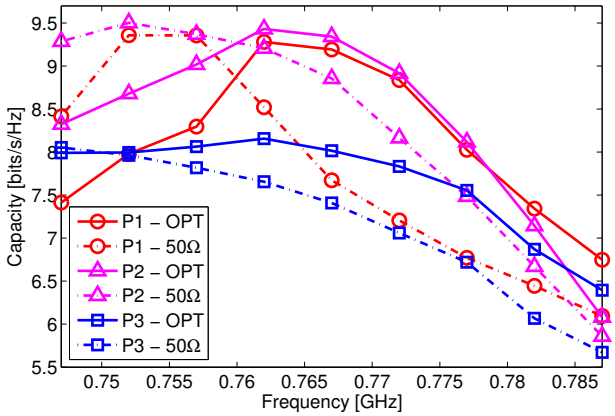

Figure 5.7: Average capacity over LTE Band 13 in the TH user scenario [17] ©2013 IEEE.

forms the optimal state, since the AIM optimization was done at the center frequency only. Therefore, on average over the full system bandwidth the AIM gain drops significantly. Hence, in practice, simultaneous impedance tuning at multiple frequency points over the system bandwidth can lead to improved AIM performance.

Experimental Verification

The analytical studies discussed above established AIM as a viable method for user effect mitigation. However, in practice, impedance tuners introduce losses that directly affect AIM gains. Hence, detailed tuner loss and coverage characterization as well as experimental verification of the AIM system is crucial.

In [50] (Paper III) the Maury mechanical tuners were applied to a TH setup with a phantom torso and yielded power gains of up to 2.1 dB in an indoor environment. Nevertheless, losses up to 0.7 dB were estimated by channel gain comparisons between the ideal lossless tuners and the Maury tuners. Hence, the result shows that overall improvements in performance are feasible in the field. However, this experiment did not tackle a real-world integrated AIM solution. More practical CMOS-SOI tuners were investigated in [51] (Paper V) where detailed measurements and tuner characterization were performed. Figure 5.8 shows the measured coverage and total tuner loss. The tuner design was exclusively optimized for the IFA terminal (Prototype 5 in Paper I) used throughout

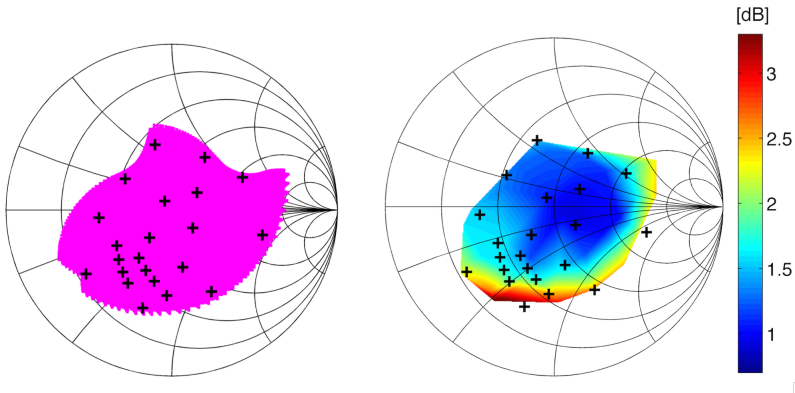

Figure 5.8: CMOS-SOI tuner measured coverage (left) and total loss (right) [51].

the study. Therefore, the coverage region was adjusted to accommodate more states with negative reactance, as previous studies with the terminal revealed that the states in this region would most effectively compensate for user interactions. The tuner has a resolution of $2^5 \times 2^5 \times 2^5 = 32768$ states (outlined by the magenta region in Fig. 5.8), whereas the black cross markers indicate the 22 states used throughout the propagation measurements. Also displayed in Fig. 5.8 is the total tuner loss measured for 39 impedance states at different VSWR according to the setup in [86]. As expected the losses increase with VSWR (1 dB at VSWR = 1 and 3.5 dB at VSWR = 4.9). This result suggests that well-matched antennas (*i.e.*, $Z_{IN} = 50\Omega$) will experience losses rather than benefits from the tuner system. Moreover, tuner loss variations with VSWR need to be considered when optimizing MIMO system performance. In general, the true potential of AIM is in cases with severe user-induced degradation such as the freestyle and firm grips tested in [51] (Paper V).

Measurements over 10 different users have shown promising AIM gain in both the freestyle and firm grips. Figure 5.9 shows the ME gain in the freestyle grip measured in a shielded room environment. Improvements from 2.5 dB (User 2) to 3.3 dB (User 3) have been recorded. Since the gain was referenced to the 50 Ω state, tuner loss variations with VSWR were inherently taken into account in the gain calculation, and only losses at the 50 Ω state (1 dB) need to the considered (dashed line in Fig. 5.9). This results in net AIM gains up to 2.3 dB in the freestyle setup. Figure 5.9 also presents the system capacity map for User 3 in the firm grip, showing capacity variation over impedance states on the Smith Chart. As expected from previous studies the optimal state for

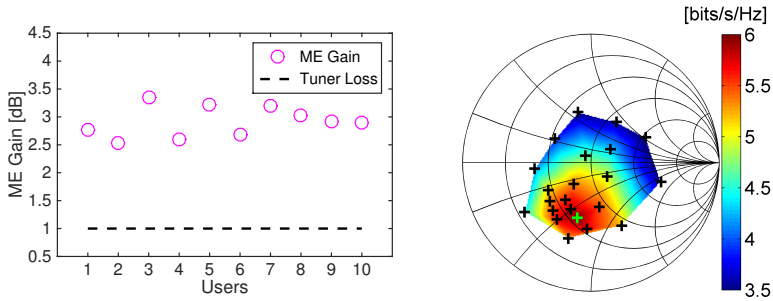

Figure 5.9: ME gain in the freestyle grip (left) and User 3 capacity map in the firm grip (right) [51].

MIMO capacity (green cross marker) has a negative reactance and is located near the antenna input impedance conjugate. However, the optimal state lies on a circle with a VSWR of 2.6, whereas the input impedance conjugate lies on a circle with a VSWR of 4.2. As discussed earlier higher VSWR implies higher loss, therefore one key conclusion here is that the optimal impedance state in practical AIM systems is the one that provides the best compromise between low tuner loss and high ME.

5.4 Antenna-Channel Harmonization

The most commonly used reference propagation environment for antenna performance evaluation is a uniform 3D APS. However, real cellular environments are often characterized by incoming power with limited angular spread (AS). In [89] the WINNER II channel model specifies measured propagation scenarios with AS between 12° and 53°. Moreover, given the random orientation of terminals during usage, narrow AS environments with random angles of incidence for the incoming power need to be investigated. Ideally, in order to maximize SNR the receive antenna radiation patterns need to spatially align (synchronize) with the incoming power originating from the transmitter antennas. In this context, the following section discusses the role AIM plays in improving antenna-channel interaction.

Simulation Studies

The study in [18] (Paper IV) investigates two terminal prototypes in four different propagation setups. Both uniform 3D APS (2.11) and a Gaussian 3D APS

(2.12) with different ASs (15°, 30°, 60°) have been tested. For each AS of the Gaussian APS a full sweep of all incident angles in both elevation ($0°<\theta<180°$) and azimuth ($-180°<\phi<180°$) was simulated. Figure 5.10 shows the spread between the maximum and minimum AIM capacity gain over all potential incident angles in each of the propagation environments. In some cases, such as the TH case for Prototype A, the capacity gain for AS = 15° changes significantly with incident angles. Variations between 35% and 50% have been recorded. Moreover, as the AS increases the gain variation reduces, converging to the uniform 3D APS case (*i.e.*, 43% gain). Therefore, AIM has higher potential in environments with a narrow AS as compared to uniform 3D cases. However, higher performance is only achieved at certain incident angles.

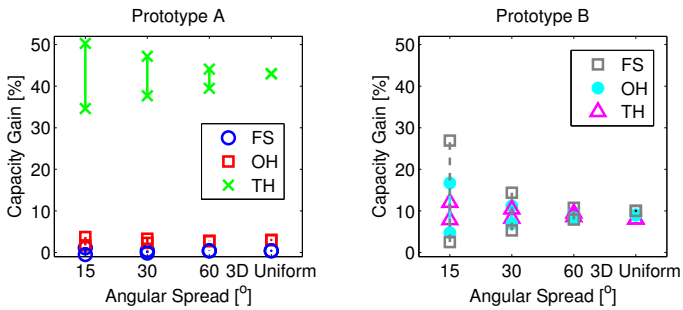

Figure 5.10: AIM capacity gain range in percentage over all incident angles and APSs - Prototype A (left) and Prototype B (right) [18].

Further analysis in [18] (Paper IV) discussed the origin of the higher AIM performance in narrow ASs. It was pointed out that due to the logarithmic dependence of MIMO capacity on SNR (2.4), different effective SNRs would lead to variations in the AIM capacity gain. From (2.4), system capacity evaluation at high SNRs would result in a higher AIM capacity gain as compared to evaluation at lower effective SNRs. In [18] (Paper IV) high effective SNRs were associated with radiation pattern maxima and vice versa for low effective SNRs. Therefore, it was established that the incident angle directions associated with maximum gain were determined by the antenna radiation pattern maxima when the tuners do not significantly influence envelope correlation (no notable radiation pattern changes). However, in cases when the AIM affected the spatial correlation performance of the terminal, the maximum gain direction was determined by the direction for which a high envelope correlation improvement was observed. Hence, it can be concluded that the effect AIM has on correlation and the spatial structure of the antenna radiation pattern determines the directions of maximum capacity gain.

Experimental Verification

Experimental verification of AIM performance in scenarios with limited AS is challenging not only due to the terminal setup with a user and real impedance tuners, but also due to the stringent requirements on the AS and incident angles of MPCs in the propagation environment. In practice, it is difficult to enforce a specific AS and angle of incidence under realistic conditions. Therefore, throughout this work we aimed at investigating environments offering significant AS variations such as LOS and NLOS setups as well as indoor and outdoor scenarios. Initial measurements in [50] (Paper III) recorded AIM power gains of 2.1 dB and 1.6 dB for an indoor and an outdoor environment, respectively. More recent propagation measurements were performed in [51] (Paper V) for a LOS, a NLOS and a shielded room (SR) environment (see Fig. 2.5). Initial observations from [50] (Paper III) were confirmed by an average ME gain difference of 0.6 dB between the LOS and SR setups in favor of the LOS scenario. In this case, unlike the setup in [50] (Paper III), the TX and RX radiation patterns were intentionally aligned in the LOS case and misaligned in the SR setup. With this approach a narrow AS was expected in the LOS scenario and a wider AS was expected in the SR case. However, the observed gain differences in the experimental verification were relatively small (up to 0.6 dB) and were within experimental errors leading to inconclusive evidence of AIM performance in narrow AS conditions. Nevertheless, these observations do not contradict the analytical studies in [18] (Paper IV). As it was argued in [51] (Paper V) channel normalization to the FS scenario led to similar effective SNRs and hence only minor AIM gain variations over different environments could be expected for the setup in [50] (Paper III) and [51] (Paper V).

5.5 Technology Demonstration

During the experimental verification measurements, discussed above, MIMO system metrics were not presented in real-time. Data was collected and stored for later evaluation and analysis. Even though this method provided detailed results, in practice the time frame for handsets to employ AIM and react to user interaction is very short. In this context, a technology demonstration was developed showing near real-time MIMO system performance.

Custom Evaluation Software

The demonstration setup was similar to the one used throughout the experimental verification measurements discussed in Chapter 5.2. However, the custom LabVIEW software was modified to perform real-time data evaluation. This required simultaneous control and synchronization between the VNA, the digital control board and the laptop used to run the software. Moreover, a MathScript RT module was implemented to execute MATLAB [76] evaluation code within the LabVIEW framework and provide MIMO system performance metrics such as capacity. These additions to the original measurement software significantly increased the software complexity.

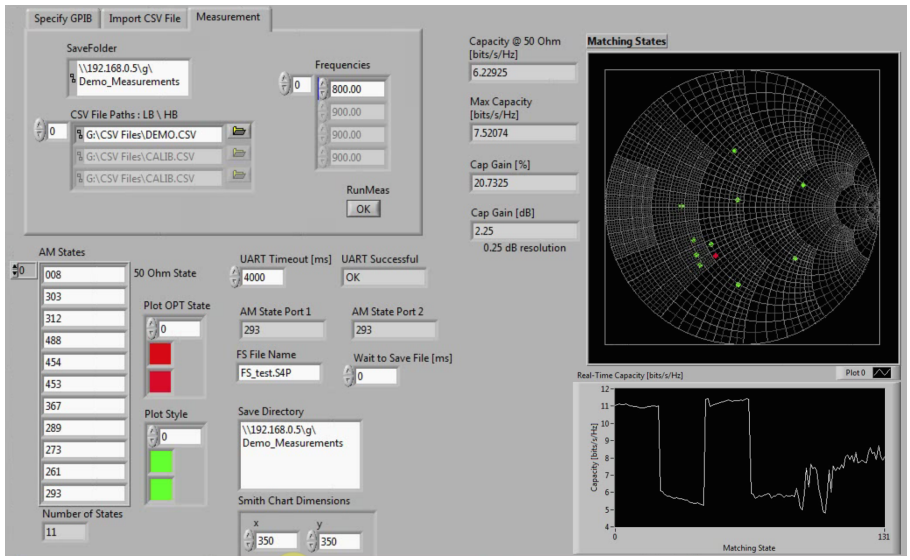

Figure 5.11: Custom LabVIEW measurement and evaluation software.

Figure. 5.11 presents a screenshot of the software after the completion of a demonstration measurement cycle. The control boxes on the left of the screen are used to set the tuner impedance states, the settings for the VNA and the file path for data storage. In this demonstration eleven tuner states were measured, where the first state in the list sets the tuners to 50 Ω as a reference for AIM gain estimation. The remaining ten states were arranged in a coarse or in a fine grid on the Smith chart depending on the measurement cycle (the coarse grid is shown in Fig. 5.11). The results from the measurement are displayed on the right hand side of the screen, where a Smith chart and a linear plot evolve in real-time to show the current tuner state measured and the evaluated MIMO capacity at that state. Throughout the capacity calculations the reference SNR was set to 20 dB. Once the measurement cycle of 11 states is completed the software analyzes the data from all states, outlines the optimal state in red and displays the AIM gain in a table format next to the Smith chart (see Fig. 5.11). A full demonstration video including a hardware setup description and a summary of the antenna-tuner performance was recorded and made public in [90].

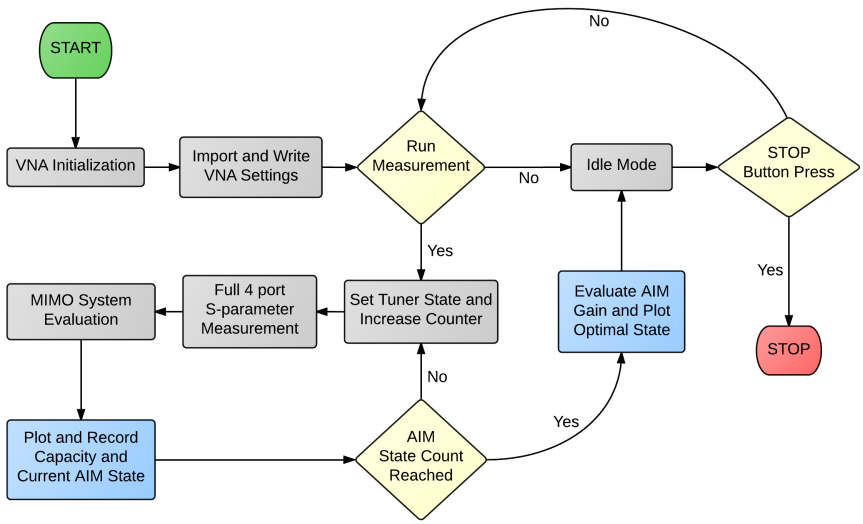

Figure 5.12: Custom LabVIEW software flowchart.

Typically, two sets of measurements are needed. The first is a quick reference measurement during which the scenario used for normalization is measured (in this case FS), whereas the second is the actual demonstration. The demonstration software flowchart is provided in Fig. 5.12. In the first stage of

the measurement the software initializes the VNA and imports settings from a previously defined file. Then by hitting the "RunMeas" button (see Fig. 5.11) a measurement cycle is initiated. During the cycle a tuner state is loaded, S parameters are measured and the recorded data is immediately analyzed and plotted. This procedure is performed for all tuner states. Once all states are evaluated the software displays the state with the best capacity performance and also outlines the AIM gain both in terms of capacity and SNR. The time needed for evaluating all 11 states depends heavily on the VNA settings. In this setup an IFBW of 2 kHz and an averaging factor of 5 were used which resulted in a total run time of 40 seconds for 11 states including capacity estimation. Optimization for the best IFBW and averaging has not been performed but it is expected to significantly reduce measurement time.

Near Real-Time Measurements

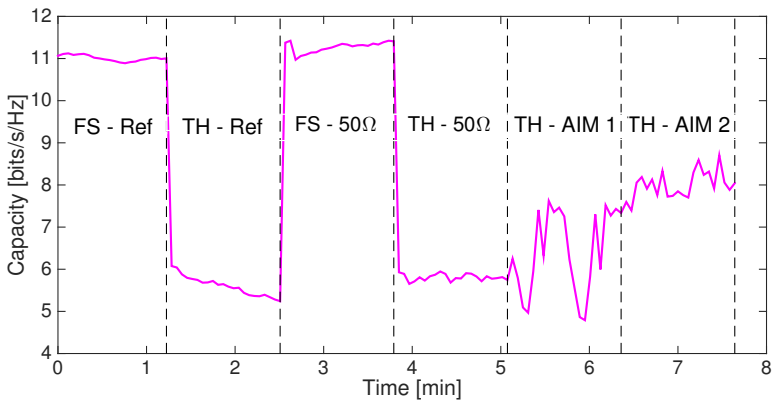

Figure 5.13: Near real-time capacity measurement at 20 dB reference SNR.

The measurement from the demonstration video in [90] is presented in Fig. 5.13. Different regions are outlined indicating a change in user grip or impedance tuner setup. Each region corresponds to two measurement cycles (11 states each) done to show valid measurement repeatability. In total, six different setups were measured. During the first two regions the reference prototype was used where the tuner PCBs were installed with a direct through connection to the antenna feed instead of the tuner chip. For the next two regions the prototype with the tuner chips on board (see Fig. 5.6) was used

where the tuners were set to the 50 Ω state throughout all 11 slots of the cycle. In the first and third regions the terminal was set up in FS, whereas in the second, fourth, fifth and sixth regions the terminal was set up in a TH scenario. Moreover, in the fifth and sixth regions the tuners were set to sweep the Smith Chart with different resolution. During the fifth region two cycles were measured with the coarse grid shown in Fig. 5.11. In the last region a finer resolution grid was tested, where the chosen states were focused around the Smith Chart region optimal for the terminal [90]. The first 5 minutes of the demonstration measurement were aimed at showing in practice the effect of the user grip on the terminal performance. Moreover, the validity of the setup was verified through multiple runs with both the reference prototype and the tuner-equipped prototype. It can be seen from the results that there are only small capacity variations (up to 0.4 bits/s/Hz) within three of the first four regions suggesting acceptably small measurement errors mainly due to the small number of samples collected in order to limit measurement time. Moreover, the nominal capacity values for the reference prototype and the prototype with tuners (set at the 50Ω state) match very well across both user scenarios. Introducing the TH grip resulted in a 46 % drop in capacity (11 bits/s/Hz to 5.9 bits/s/Hz) confirming the severe user-induced degradation discussed in previous chapters. In the last 2.5 minutes of the measurement the impedance tuners were used to improve system performance. During the coarse grid runs the optimal capacity reached 7.5 bits/s/Hz (27 % increase compared to the 50 Ω state). Furthermore, when a finer resolution grid was applied capacity of up to 8.7 bits/s/Hz was measured resulting in a capacity gain of up to 47 %. Therefore, the performed demonstration confirms our initial expectations and shows the vast potential of AIM to mitigate user effects in a near real-time measurement.

Chapter 6

Research Contributions

This chapter provides a brief summary of the included papers and highlights the main research contributions of the thesis.

6.1 Paper I: "On User Effects in MIMO Handset Antennas Designed Using Characteristic Modes"

In recent years TCM has proven to be a very promising strategy for designing efficient terminal antennas for MIMO applications. This study is mainly motivated by the lack of contributions investigating user effects for TCM-based handset antennas. The paper focuses on exploring the potential of applying specific antenna designs to mitigate user interaction. Five dual-antenna MIMO prototypes from existing literature were investigated. Two of the designs were based on TCM, whereas the remaining three used more conventional antenna elements such as PIFA and monopole. In order to address the increasing variety of usage scenarios we proposed 11 representative cases designed to accommodate current smartphone form factors and to include novel hand grips. Moreover, weighted usage performance over different user scenarios was evaluated in order to take into account the dominance of certain grip styles in real usage.

In this context, the study identified the main user induced loss mechanisms for both the conventional designs and the TCM-based designs. It was established that the superior envelope correlation as well as the high matching and coupling efficiency allowed both TCM-based prototypes to outperform conventional designs in data user scenarios (as well as in the free-space case). However,

in the talk modes the correlation advantage of the TCM designs was reduced by the improved correlation in the conventional designs, leading to lower MEs for the TCM designs compared to the conventional designs. Furthermore, it was observed that due to efficient ground plane utilization both TCM-based prototypes showed distributed near fields along the entire chassis. As a result a smaller separation between the user and the closest near-field hot spot was recorded leading to higher absorption losses. Nevertheless, the weighted usage evaluation suggested that the TCM designs can outperform the conventional designs by up to 1.7 dB. Hence, it was concluded that TCM is a promising terminal antenna design strategy for reducing user effects.

I am the main contributor to this paper. I have been involved in all parts of the scientific work, including user scenario formulation and design, terminal antenna simulations, experimental verification, as well as numerical data analysis and manuscript writing.

6.2 Paper II: "Adaptive Impedance Matching Performance of MIMO Terminals with Different Bandwidth and Isolation Properties in Realistic User Scenarios"

Apart from robust antenna design, another approach for improving antenna performance by mitigating user effects is to use external impedance matching networks. More recently, adaptive impedance matching (AIM) has been proposed to combat variations due to different user scenarios. However, most studies have focused on single antenna optimization and do not provide knowledge on the AIM gain mechanisms in the context of MIMO handset antennas. This paper aims to determine the achievable MIMO system improvement as well as to gain useful insights for practical implementations of AIM.

The study employed a variable lossless impedance matching network consisting of a transmission line and an open circuited stub. AIM was applied to three terminal prototypes with different antenna isolation and bandwidth. The target frequency bands were LTE Band 13 and LTE Band 7, though the focus of this work was in the lower band (LTE Band 13) where terminal design is more challenging. Capacity results for 4 user scenarios at the center frequency as well as averaged over the entire band were presented. For the narrowband case it was concluded that the terminal with the smallest antenna bandwidth could benefit the most from AIM. However, the AIM gain decreased when the results were averaged over the entire bandwidth, as the adaptive matching networks can provide good matching only for a limited bandwidth. Overall,

the prototype with moderate bandwidth and isolation showed the highest AIM gain over LTE Band 13, emphasizing the significant impact of bandwidth and isolation on AIM performance.

This work was chosen among 180 student papers as one of the 10 finalists for the Young Scientist Award at the European Conference on Antennas and Propagation (EuCAP) 2013. I am the main contributor to the paper. I have been involved in all parts of the scientific work, including AIM model implementation, user scenarios design, terminal antenna simulations as well as numerical data analysis and manuscript writing.

6.3 Paper III: "Measured Adaptive Matching Performance of a MIMO Terminal with User Effects"

The study in Paper II has shown very promising initial results on the potential of AIM to compensate for user induced degradation in the context of MIMO terminals. However, practical verification in realistic propagation and user scenarios is a vital step towards understanding the full potential of AIM. This paper presents an experiment conducted with real impedance tuners in both an indoor and an outdoor propagation environment, which significantly extended the previous work in Paper II.

This study focused on three user scenarios including both phantom hands and a torso phantom. Two Maury mechanical tuners controlled in LabView to sweep predefined areas in the Smith chart were used for the AIM implementation. Capacity results from the two propagation environments were presented revealing differences in AIM gain for the two environments. Higher AIM power gain was established for the indoor scenario (2.1 dB) as compared to the outdoor case (1.6 dB). Moreover, the paper evaluated impedance tuner losses and discussed their impact on the overall performance. It was concluded that even in the presence of realistic AIM networks significant gains are feasible over a standard 50 Ω termination (*i.e.*, no AIM).

This work was carried out in cooperation with Sony Mobile Communications AB in Lund who provided valuable measurement equipment and expert advice on the setup and data analysis. I am the main contributor to this paper. I have been involved in all parts of the scientific work, including propagation measurement setup and execution as well as data analysis and manuscript writing.

6.4 Paper IV: "Impact of Antenna Design on MIMO Performance for Compact Terminals with Adaptive Impedance Matching"

The observations in Paper III revealed interesting results regarding the potential of AIM in different propagation scenarios. However, a more detailed investigation was necessary in order to determine the underlying mechanisms behind AIM performance in various conditions. This concern was addressed here with a detailed comparison on the AIM performance of two MIMO terminal prototypes with fundamentally different antenna designs. The main goal was to determine the impact of antenna design on AIM performance as well as to do a comprehensive study involving several propagation conditions.

The two terminals investigated here have the same form factor, but provided significantly different bandwidth, isolation, and matching properties due to the use of different antenna types and location. The three user scenarios studied were similar to Paper III, however the half-body phantom was excluded. The complete AIM model from Paper II was used, but instead of simulated antenna parameters, measured antenna radiation patterns, efficiencies and scattering parameters were employed. Moreover, the propagation model assumed both uniform 3D APS and Gaussian 3D APS, where four different angular spreads (ASs) were investigated for the Gaussian APS with all possible incident angle directions.

Apart from the AIM network achieving capacity gains of up to 50%, detailed discussions outlined several key trends. Antenna location significantly affected user induced losses, consequently AIM performance. Moreover, this study extended the work in Paper II by comparing terminals with a much larger difference in bandwidth. As a result it was established that the wider bandwidth prototype was less susceptible to user interaction and therefore exhibited lower AIM gains. Nevertheless, a tradeoff in impedance matching was needed to achieve a wide bandwidth, which meant that AIM could provide this prototype with additional matching to increase efficiency even in FS. Therefore, it was concluded that the more user robust wideband design could also significantly benefit from employing impedance tuners. Moreover, an exhaustive search over 96 impedance states revealed that optimal capacity states did not necessarily correspond to the states for maximum received power, which emphasized that AIM gain could involve a fundamental tradeoff between received signal power and correlation.

Furthermore, it was found that a narrow AS may lead to a higher AIM gain compared to the 3D uniform APS. However, it was highlighted that AIM performance in narrow ASs was very sensitive to the incident angle direction.

Spatial regions of high AIM gain in narrow AS conditions corresponded to antenna radiation pattern maxima or minima depending on the effect AIM has on the envelope correlation.

This work was carried out in cooperation with Sony Mobile Communications AB in Lund where the terminal prototypes were measured in a SATIMO Stargate measurement facility. I am the main contributor to this paper. I have been involved in all parts of the scientific work, including AIM model development, propagation modeling, antenna optimization, manufacturing, and measurement as well as data analysis and manuscript writing.

6.5 Paper V: "Experimental Investigation of Adaptive Impedance Matching for a MIMO Terminal under Realistic Conditions"

Even though significant efforts have been invested on measurements with AIM equipped terminal devices, to our knowledge no study has looked into the performance of MIMO terminals with integrated tuners in real-life propagation conditions. Moreover, recent studies have expressed serious concerns on the validity of user phantom models compared to real test subjects. In fact, a few papers have shown significant differences in the results, both in terms of impedance mismatch and absorption loss. In this context, we were motivated to develop a terminal-integrated solution for AIM and evaluate its performance in realistic user conditions with both test subjects and phantom hands.

The final paper in this thesis investigated practical aspects of AIM not explored in other included papers and was the result of a successful collaboration between two research groups and two companies. Two custom designed CMOS-SOI impedance tuners with state of the art linearity, power handling and impedance state coverage were used to build a dual-antenna terminal prototype with AIM. Custom LabView software was developed to control the impedance tuners and the propagation measurement setup as well as to evaluate MIMO system performance. Furthermore, the AIM setup was measured in three different propagation environments, whereas several different hand grips were studied. Two of the grips were measured for 10 test subjects.

The study reported net AIM gain based on the use of realistic tuners. Significant performance improvements were recorded for both a freestyle and a firm grip. The AIM gains were mainly due to improved received power (up to 3 dB net gain). Moreover, the validity of the concerns about differences between user phantoms and real test subjects was confirmed. The differences were mainly attributed to the limited flexibility of phantom hands to reproduce

realistic grips for large terminal form factors. Additionally, a sweep through 22 impedance states established that the optimal capacity states did not correspond to the complex conjugate of the input impedance for the terminal antenna due to the insertion losses of the tuner chips. The optimal state observed in each setup represented a tradeoff between low insertion loss and high antenna total efficiency. Moreover, some differences in the net AIM gains were reported for the different propagation environments, supporting the observations in Paper III. However, the differences were relatively small (up to 0.6 dB) and could be accounted for by experimental tolerances. Therefore, the paper revealed no strong dependence of AIM gain on the propagation channel in the case of the tuner-equipped prototype.

This work was carried out in cooperation with Sony Mobile Communications AB in Lund who provided part of the measurement equipment as well as STMicroelectronics AB in Lund who manufactured the tuner chips. I am the main contributor to this paper. I have been involved in all parts of the scientific work, including tuner characterization, MIMO prototype manufacturing, propagation measurements planning and execution as well as data analysis and manuscript writing.

Chapter 7

Conclusions and Outlook

Wireless transmission can benefit substantially from highly efficient antennas. For most applications the contradictory requirements on size and bandwidth significantly complicate the antenna design process. However, in the context of mobile handsets, one of the most challenging problems is user induced antenna performance degradation. The inevitable absorption of electromagnetic waves in the body of the user as well as antenna impedance mismatch result in severe power loss and consequently lower SNR. The implementation of MIMO technology in the last decade further increased complexity by posing additional requirements on the number of antenna elements per terminal for the same handset volume as well as on the correlation among all antenna pairs. This thesis investigates potential solutions for mitigating user effects. An interdisciplinary approach was used combining the fields of antennas, propagation and circuit design to offer useful insights on user robust MIMO terminal antenna systems.

It is known that different antenna types and general design strategies can lead to significant performance differences for handsets in the presence of a user. Recent terminal designs based on TCM have shown excellent performance in FS. However, more relevant user cases such as talk and data modes have not been investigated in detail. Paper I in this thesis addresses these scenarios by exploring both conventional terminal designs and more recent TCM-based designs in order to gain additional insight on user robust design strategies. The main results revealed that prototypes optimized with TCM showed higher multiplexing efficiencies (MEs) in most data mode scenarios as a result of higher matching and coupling efficiencies as well as significant correlation advantages relative to the conventional designs. However, additional analysis on near-field interaction suggested that the more distributed near-fields of the TCM opti-

mized antennas can lead to higher absorption losses. Nevertheless, by weighting the antenna performance according to usage behavior, it has been shown that the TCM designs outperform more conventional terminals by at least 1.1 dB, indicating that TCM is a promising strategy for designing user robust handset antennas.

Traditionally, external matching components are regularly used to improve antenna efficiency. Studies have also shown this to be a viable strategy to compensate for impedance mismatch due to user proximity. However, with rapid evolution of smartphone form factors and usage scenarios, it is very difficult to predict the antenna impedance in the presence of users. Recently, adaptive impedance matching (AIM) was proposed as a potential solution to this problem. A closed-loop AIM system is capable of sensing the antenna impedance and re-matching it for higher efficiency by employing variable matching components. However, only a few contributions have thus far investigated the application of AIM to multi-antenna terminals. Moreover, experimental verification of AIM systems in realistic propagation and user conditions remains a relatively unexplored area. The major part of this thesis investigates the potential of AIM to improve MIMO system performance, focusing on extending existing knowledge on the achievable performance gain and the gain mechanisms in different operating conditions. Moreover, one of the main goals of this thesis was to develop and build a complete AIM system and demonstrate its potential to both academia and industry.

In this context, Papers II-V are dedicated to AIM. The study began by building a simulation tool for evaluating system performance of MIMO terminals with ideal, lossless AIM as well as simulated users, antennas, and channels. Subsequent studies progressively relaxed the ideal assumptions in order to evaluate practical aspects of applying AIM. Significant AIM gains were recorded in a variety of user scenarios and propagation conditions both for lossless and realistic impedance tuners. In most of the cases optimal MIMO system performance was achieved by a tradeoff between optimal received power and envelope correlation. Tuner losses were taken into account in the practical implementations in Paper III and Paper V in order to estimate net AIM gains. It was emphasized that in cases of severe impedance mismatch the optimal states were the result of a tradeoff between low tuner losses and high antenna total efficiency. Moreover, variations of AIM performance were observed for propagation conditions with different AS. Narrow AS environments have the potential to result in higher AIM gains depending on the incident angle of incoming multipath components. Furthermore, terminal designs with narrow and wide bandwidths were investigated, indicating that narrowband antennas are more susceptible to user interaction and hence have higher AIM gains. Nevertheless, due to poorer impedance matching at resonance, wide bandwidth terminals

can also benefit from AIM systems. Finally, the development of a technology demonstrator was discussed. In the thesis overview near real-time MIMO performance improvement, as obtained by the demonstrator, was described. Therefore, the thesis concludes that impedance tuners can play a vital role in future communication systems and have the potential to significantly reduce user-induced losses.

Possible future work in the area includes more refined methods for user effect mitigation. First, TCM-based terminal designs can be improved by optimizing the interaction between radiation modes and the user. This approach is expected to yield large improvements over the current strategy of designing TCM-based antennas in free space. Moreover, impedance tuners with reduced insertion losses and wider coverage could enhance AIM potential beyond the results presented in this thesis. Furthermore, the algorithm for performing AIM was not explicitly considered in this thesis work, where a sweep of relevant states was performed. Therefore, more efficient algorithms as well as realistic impedance detectors are also an interesting aspect for future studies. Finally, recent developments in wearable technology suggest novel types of wrist-oriented terminal devices operating on cellular networks. This unexplored area presents new exciting research opportunities on investigating user effect mitigation techniques for an entirely different form factor and user scenario.

References

[1] T. S. Rappaport, *Wireless Communications.* Prentice Hall PTR, 2002.

[2] http://www.bloomberg.com/bw/articles/2012-06-29/before-iphone-and-android-came-simon-the-first-smartphone/

[3] http://research.microsoft.com/en-us/um/people/bibuxton/buxtoncollection/detail.aspx?id=40

[4] http://www.statista.com/statistics/263441/global-smartphone-shipments-forecast/

[5] A. Osseinran, et al., "Scenarios for 5G mobile and wireless communications: the vision of the METIS project," *IEEE Communications Magazine,* vol. 52, no. 5, pp. 26-35, May 2014.

[6] E. Hossain, M. Rasti, H. Tabassum, and A. Abdelnasser, "Evolution toward 5G multi-tier cellular wireless networks: an interference management perspective," *IEEE Wireless Communications Magazine,* vol. 21, no. 3, pp. 118-127, Jun. 2014.

[7] J. G. Andrews, et al., "What will 5G be?," *IEEE Journal on Selected Areas in Communications,* vol. 32, no. 6, pp. 1065-1082, Jun. 2014.

[8] F. Boccardi et al., "Multiple-antenna techniques in LTE-Advanced," *IEEE Communications Magazine,* vol. 50, no. 3, pp. 114-121, Mar. 2012.

[9] R. Vaughan and J. B. Andersen, *Channels, Propagation and Antennas for Mobile Communications.* London, U.K.: Inst. Elect. Eng., 2003.

[10] A. v. Bezooijen, R. Mahmoudi, and A. v. Roermund, *Adaptive RF Front-Ends for Hand-held Applications.* London, U.K.: Springer, 2011.

[11] M. A. Jensen and J. W. Wallace, "A review of antennas and propagation for MIMO wireless communications," *IEEE Transactions on Antennas and Propagation,* vol. 52, no. 11, pp. 2810-2824, Nov. 2004.

[12] A. Paulraj, R. Nabar, and D. Gore, *Introduction to Space-Time Wireless Communications.* New York, U.S.: Cambridge University Press, 2003.

[13] G. J. Foschini and M. J. Gans, "On limits of wireless communications in a fading environment when using multiple antennas," *Wireless Personal Communications,* vol. 6, pp. 311-335, 1998.

[14] N. Costa and S. Haykin, *Multiple-Input Multiple-Output Channel Models.* New Jersey, U.S.: John Wiley & Sons, 2010.

[15] A. F. Molisch, *Wireless Communications.* Wiley-IEEE Press, 2005.

[16] H. Özcelik, M. Herdin, W. Weichselberger, J. Wallace, and E. Bonek, "Deficiencies of Kronecker MIMO radio channel model," *Electronics Letters,* vol. 39, pp. 1209-1210, Aug. 2003.

[17] I. Vasilev, E. Foroozanfard, and B. K. Lau, "Adaptive impedance matching performance of MIMO terminals with different bandwidth and isolation properties in realistic user scenarios," in *Proc. European Conference on Antennas and Propagation,* Gothenburg, Sweden, Apr. 8-12, 2013, pp. 2516-2520.

[18] I. Vasilev, V. Plicanic, and B. K. Lau, "Impact of antenna design on MIMO performance for compact terminals with adaptive impedance matching," in revision for *IEEE Transactions on Antennas and Propagation,* Jun. 2014.

[19] T. Taga, "Analysis for mean effective gain of mobile antennas in land mobile radio environments," *IEEE Transactions on Vehicular Technology,* vol. 39, pp. 117-131, May 1990.

[20] R. Tian, B. K. Lau, and Z. Ying, "Multiplexing efficiency of MIMO antennas in arbitrary propagation scenarios," in *Proc. European Conference on Antennas and Propagation,* Prague, Czech Republic, Mar. 26-30, 2012, pp. 373-377.

[21] M. B. Knudsen and G. F. Pedersen, "Spherical outdoor to indoor power spectrum model at the mobile terminal," *IEEE Journal on Selected Areas in Communications,* vol. 20, no. 6, pp. 1156-1169, Aug. 2002.

[22] R. Tian, "Design and evaluation of compact multi-antennas for efficient MIMO communications," *PhD Thesis,* Department of Electrical and Information Technology, Lund University, Sweden, 2011.

[23] J. Salo, P. Suvikunnas, H. M. El-Sallabi, and P. Vainikainen, "Some results on MIMO mutual information: the high SNR case," in *Proc. IEEE Global Telecommunications Conference,* Dallas, TX, 2004, pp. 943-947.

[24] J. Salo, P. Suvikunnas, H. M. El-Sallabi, and P. Vainikainen, "Ellipticity statistic as a measure of MIMO multipath richness," *Electronics Letters,* vol. 42, no. 3, Feb. 2006, pp. 45-46.

[25] V. Plicanic, "Characterization and enhancement of antenna system performance in compact MIMO terminals," *PhD Thesis,* Department of Electrical and Information Technology, Lund University, Sweden, 2011.

[26] R. Tian, B. K. Lau, and Z. Ying, "Multiplexing efficiency of MIMO antennas," *IEEE Antennas and Wireless Propagation Letters,* vol. 10, pp. 183-186, 2011.

[27] T. Abbas, "Measurement based channel characterization and modeling for vehicle-to-vehicle communications," *PhD Thesis,* Department of Electrical and Information Technology, Lund University, Sweden, 2014.

[28] R. Tian, V. Plicanic, B. K. Lau, and Z. Ying, "A compact six-port dielectric resonator antenna array: MIMO channel measurements and performance analysis," *IEEE Transactions on Antennas and Propagation,* vol. 58, no. 4, pp. 1369-1379, Apr. 2010.

[29] http://www.3gpp.org/

[30] D. D. Falconer, F. Adachi, and B. Gudmundsson, "Time division multiple access methods for wireless personal communications," *IEEE Communications Magazine,* vol. 33, no. 1, pp. 50-57. 1995.

[31] "CTIA test plan for wireless device over-the-air performance," Revision 3.3.2, CTIA Wireless Association, Sep. 2014.

[32] "Cisco visual networking index: global mobile data traffic forecast update, 2013-2018," White Paper, Feb. 2014.

[33] B. K. Lau, "Multiple antenna terminals," in *MIMO: From Theory to Implementation,* C. Oestges, A. Sibille, and A. Zanella, Eds. San Diego, CA, USA: Academic, 2011 pp. 267-298.

[34] https://www.apple.com/se/iphone-6/specs/

[35] L. J. Chu, "Physical limitations of omni-directional antennas," *Journal of Applied Physics,* vol. 19, no. 12, pp. 1163-1175, Dec. 1948.

[36] M. Gustafsson, C. Sohl, and G. Kristensson, "Illustrations of new physical bounds on linearly polarized antennas," *IEEE Transactions on Antennas and Propagation,* vol. 57, no. 5, pp. 1319-1327, May 2009.

[37] H. Li, Z. Miers, and B. K. Lau, "Design of orthogonal MIMO handset antennas based on characteristic mode manipulation at frequency bands below 1 GHz," *IEEE Transactions on Antennas and Propagation,* vol. 62, no. 5, pp. 2756-2766, Feb. 2014.

[38] J. Toftgård, S. N. Hornsleth, and J. B. Andersen, "Effects on portable antennas of the presence of a person," *IEEE Transactions on Antennas and Propagation,* vol. 41, no. 6, pp. 739-746, Jun. 1993.

[39] M. A. Jensen and Y. Rahmat-Samii, "EM interaction of handset antennas and a human in personal communications," *Proceedings of the IEEE,* vol. 83, no. 1, pp. 7-17, Jan. 1995.

[40] G. F. Pedersen, J. Ø. Nielsen, K. Olesen, and I. Z. Kovacs, "Measured variation in performance of handheld antennas for a large number of test persons," in *Proc. IEEE Vehicular Technology Conference,* vol. 1, Ottawa, Canada, May 18-21, 1998, pp. 505-509.

[41] G. F. Pedersen, K. Olesen, and S. L. Larsen, "Bodyloss for handheld phones," in *Proc. IEEE Vehicular Technology Conference,* vol. 2, Houston, TX, May 16-20, 1999, pp. 1580-1584.

[42] K. R. Boyle, Y. Yuan, and L. P. Ligthart, "Analysis of mobile phone antenna impedance variations with user proximity," *IEEE Transactions on Antennas and Propagation,* vol. 55, no. 2, pp. 364-372, Feb. 2007.

[43] M. Webb, D. Gibbins, and M. Beach, "Slot antenna performance and signal quality in a smartphone prototype," *IEEE Antennas and Wireless Propagation Letters,* vol. 9, pp. 1053-1056, 2010.

[44] A. A. H. Azremi, K. Haneda, and P. Vainikainen, "Site-specific evaluation of a MIMO channel capacity for multi-antenna mobile terminals in proximity to a human hand," in *Proc. European Conference on Antennas and Propagation,* Rome, Italy, Apr. 11-15, 2011, pp. 538-542.

[45] M. Pelosi, O. Franek, M. B. Knudsen, M. Christensen, and G. F. Pedersen, "A grip study for talk and data modes in mobile phones," *IEEE Transactions on Antennas and Propagation,* vol. 57, no. 4, pp. 856-865, Apr. 2009.

[46] http://www.indexsar.com/index-phantomhands.html

[47] http://www.speag.com/products/em-phantom/hand/

[48] S. Hoober, "How do users really hold mobile devices?," Feb. 2013, http://www.uxmatters.com/mt/archives/2013/02/how-do-users-really-hold-mobile-devices.php

[49] I. Vasilev and B. K. Lau, "On user effects in MIMO handset antennas designed using characteristic modes," submitted to *IEEE Antennas Wireless Propagation Letters,* Mar. 2015.

[50] I. Vasilev, V. Plicanic, and B. K. Lau, "Measured adaptive matching performance of a MIMO terminal with user effects," *IEEE Antennas Wireless Propagation Letters,* pp. 1720-1723, 2013.

[51] I. Vasilev, J. Lindstrand, V. Plicanic, H. Sjöland, and B. K. Lau, "Experimental investigation of adaptive impedance matching for a MIMO terminal under realistic conditions," submitted to *IEEE Transactions on Antennas and Propagation*, Mar. 2015.

[52] K. R. Boyle, "The performance of GSM 900 antennas in the presence of people and phantoms," in *Proc. International Conference on Antennas and Propagation,* Exeter, UK, Mar. 31 - Apr. 3, 2003, pp. 35-38.

[53] K. R. Boyle, E. Spits, M. de Jongh, S. Sato, T. Bakker, and A. van Bezooijen, "Gain statistics for mobile phone antenna tuners," in *Proc. European Conference on Antennas and Propagation,* Gothenburg, Sweden, Apr. 8-12, 2013, pp. 432-436.

[54] V. Plicanic, I. Vasilev, R. Tian, and B. K. Lau, "Capacity maximisation of handheld MIMO terminal with adaptive matching in indoor environment," *Electronics Letters,* vol. 47, no. 16, pp. 900-901, Aug. 2011.

[55] R. Valkonen, J. Ilvonen, K. Rasilainen, J. Holopainen, C. Icheln, and P. Vainikainen, "Avoiding the interaction between hand and capacitive coupling element based mobile terminal antenna," in *Proc. European Conference on Antennas and Propagation,* Rome, Italy, Apr. 11-15, 2011, pp. 2781-2785.

[56] J. Ilvonen, R. Valkonen, J. Holopainen, O. Kivekas, and P. Vainikainen, "Reducing the interaction between user and mobile terminal antenna based on antenna shielding," in *Proc. European Conference on Antennas and Propagation,* Prague, Czech Republic, Mar. 26-30, 2012, pp. 1889-1893.

[57] S. C. Del Barrio, I. B. Bonev, M. Pelosi, O. Franek, and G. F. Pedersen, "Reduction of the absorption loss in the head via a metamaterial inspired Z antenna," in *Proc. European Conference on Antennas and Propagation,* Rome, Italy, Apr. 11-15, 2011, pp. 2313-2317.

[58] E. Buskgaard, A. Tatomirescu, S. C. Del Barrio, O. Franek, and G. F. Pedersen, "Effect of antenna bandwidth and placement on the robustness to user interaction," in *Proc. International Workshop on Antenna Technology,* Sidney, Australia, Mar. 4-6, 2014, pp. 258-261.

[59] R. F. Harrington and J. R. Mautz, "Computation of characteristic modes for conducting bodies," *IEEE Transactions on Antennas and Propagation,* vol. AP-19, no. 5, pp. 629-639, Sep. 1971.

[60] R. Martens and D. Manteuffel, "Systematic design method of a mobile multiple antenna system using the theory of characteristic modes," *IET Microwaves, Antennas and Propagation,* vol. 8, no. 12, pp. 887-893, 2014.

[61] I. Szini, A. Tatomirescu, and G. F. Pedersen, "On small terminal MIMO antennas, harmonizing characteristic modes with ground plane geometry," *IEEE Transactions on Antennas and Propagation,* to appear, Feb. 2015.

[62] Z. Miers, H. Li, and B. K. Lau, "Design of bandwidth-enhanced and multiband MIMO antennas using characteristic modes," *IEEE Antennas and Wireless Propagation Letters,* pp. 1696-1699, 2013.

[63] Z. Miers, H. Li, and B. K. Lau, "Design of bezel antennas for multiband MIMO terminals using characteristic modes," in *Proc. European Conference on Antennas and Propagation,* The Hague, Netherlands, Apr. 6-11, 2014, pp. 2556-2560.

[64] A. Tsiaras, "SAR evaluation in multi-antenna mobile handsets," *M.Sc. Thesis,* Department of Electrical and Information Technology, Lund University, Sweden, 2014.

[65] http://www.satimo.com/content/products/sg-64

[66] J. A. Wallace and M. A. Jensen, "Termination-dependent diversity performance of coupled antennas: network theory analysis," *IEEE Transactions on Antennas and Propagation,* vol. 52, no. 1, pp. 98-105, Jan. 2004.

[67] J. A. Wallace and M. A. Jensen, "Mutual coupling in MIMO wireless systems: a rigorous network theory analysis," *IEEE Transactions on Wireless Communications,* vol. 3, no. 4, pp. 1317-1325, Jul. 2004.

[68] J. B. Andersen and B. K. Lau, "On closely coupled dipoles in a random field," *IEEE Antennas and Wireless Propagation Letters,* vol. 5, pp.73-75, 2006.

[69] Y. Fei, Y. Fan, B. K. Lau, and J. S. Thompson, "Optimal single-port matching impedance for capacity maximization in compact MIMO arrays," *IEEE Transactions on Antennas and Propagation,* vol. 56, no. 11, pp. 3566-3575, Nov. 2008.

[70] K. Karlsson, J. Carlsson, I. Belov, G. Nilsson, and P.-S. Kildal, "Optimization of antenna diversity gain by combining full-wave and circuit simulations," in *Proc. European Conference on Antennas and Propagation,* Edinburgh, UK, Nov. 11-16, 2007, pp. 1-5.

[71] K. Karlsson, "Embedded element patterns in combination with circuit simulations for multi-port antenna analysis," *PhD Thesis,* Department of Signals and Systems, Chalmers University of Technology, Gothenburg, Sweden, 2009.

[72] K. Karlsson and J. Carlsson, "Analysis and optimization of MIMO capacity by using circuit simulation and embedded element patterns from full-wave simulation," in *Proc. International Workshop on Antennas and Propagation,* Lisbon, Portugal, Mar. 1-3, 2010, pp. 1-4.

[73] B. K. Lau, J. B. Andersen, A. F. Molisch, and G. Kristensson, "Antenna matching for capacity maximization in compact MIMO systems," in *Proc. International Symposium on Wireless Communication Systems,* Valencia, Spain, Sep. 6-8, 2006, pp. 253-257.

[74] M. A. Jensen and B. K. Lau, "Uncoupled matching for active and passive impedances of coupled arrays in MIMO systems," *IEEE Transactions on Antennas and Propagation,* vol. 58, no. 10, pp. 3336-3343, Oct. 2010.

[75] R. Mohammadkhani and J. S. Thompson, "Adaptive uncoupled termination for coupled arrays in MIMO systems," *IEEE Transactions on Antennas and Propagation,* vol. 61, no. 8, pp. 4284-4295, Aug. 2013.

[76] http://se.mathworks.com/products/matlab/

[77] http://www.ni.com/labview/

[78] Y. Morandini et al., "Digitally tuning capacitor: from RF to millimeter wave applications in advanced CMOS technologies," invited talk in *European Solid-State Device Research Conference,* Bordeaux, France, Sep. 17-21, 2012.

[79] G. M. Rebeiz and J. B. Muldavin, "RF MEMS switches and switch circuits," *IEEE Microwave Magazine,* vol. 2, no. 4, pp. 59-71, Dec. 2001.

[80] P. Sjöblom and H. Sjöland, "Characterization of CMOS impedance tuning unit for DVB-H," *Analog Integrated Circuits and Signal Processing,* vol. 52, no. 3, pp. 79-87, Sep. 2007.

[81] A. van Bezooijen, M. A. de Jongh, C. Chanlo, L. C. H. Ruijs, F. van Straten, R. Mahmoudi, and A. H. M. van Roermund, "A GSM/EDGE/WCDMA adaptive series-LC matching network using RF-MEMS switches," *IEEE Journal of Solid-State Circuits,* vol. 43, no. 10, pp. 2259-2268, Oct. 2008.

[82] M. A. de Jongh, A. van Bezooijen, K. R. Boyle, and T. Bakker, "Mobile phone performance improvements using an adaptively controlled antenna tuner," in *Proc. Microwave Theory and Techniques Symposium,* Baltimore, MD, Jun. 5-10, 2011, pp. 1-4.

[83] A. S. Morris III, Q. Gu, M. Ozkar, and S. P. Natarajan, "High performance tuners for handsets," in *Proc. Microwave Theory and Techniques Symposium,* Baltimore, MD, Jun. 5-10, 2011, pp. 1-4.

[84] F. Sonnerat, R. Pilard, F. Gianesello, F. Le Pennec, C. Person, and D. Gloria, "Innovative tunable antenna solutions using CMOS SOI technology," in *Proc. International Silicon-on-Insulator Conference,* Napa, CA, Oct. 1-4, 2012, pp. 1-2.

[85] F. Sonnerat et al., "30 dBm P1dB and 4 dB insertion losses optimized 4G antenna tuner fully integrated in a 130nm CMOS SOI technology," in *Proc. Radio and Wireless Symposium,* Austin, TX, Jan. 20-23, 2013, pp. 73-75.

[86] J. Lindstrand, I. Vasilev, and H. Sjöland, "A low band cellular terminal antenna impedance tuner in 130nm CMOS-SOI technology," in *Proc. European Solid-State Circuit Conference,* Venice, Italy, Sep. 22-26, 2014, pp. 459-462.

[87] https://www.maurymw.com/MW_RF/Automated_Tuners.php

[88] http://www.atmel.com/devices/ATMEGA32.aspx

[89] IST-WINNER D1.1.2 P. Kyösti, et al., "WINNER II channel models," ver. 1.1, Sep. 2007.

[90] https://www.youtube.com/watch?v=FnHukmr8Hio&feature=youtu.be